CAVITY MEDIATED SPIN-1 ATOM INTERACTIONS

A Thesis

by

CHRISTOPHER M. LANGLETT

Submitted to the Office of Graduate and Professional Studies of
Texas A&M University
in partial fulfillment of the requirements for the degree of

MASTER OF SCIENCE

Chair of Committee,	Girish Agarwal
Committee Members,	M.Suhail Zubairy
	Robert D. Nevels
Head of Department,	Grigory Rogachev

December 2020

Major Subject: Physics

ABSTRACT

In this thesis a theoretical framework for a spin-1 exchange dynamics is developed by the use of effective Hamiltonian theory. We develop this framework through several applications beginning with the standard Jaynes-Cummings model, which under the method of time-averaging leads to the Hamiltonian described by one-axis twisting in a more efficient manner than standard adiabatic elimination. The process of developing effective many-body spin Hamiltonian's is then applied in several contexts. The robustness of the systems we studied are demonstrated through the generation of entangled states under various constraints.

We find that when fixed within a sub-manifold of the collective angular momentum states the time evolution of minimally uncertain atomic states results in atomic cat states, which have been utilized in a variety of contexts for precision measurements. More so, when the initial state is given freedom to evolve between all angular momentum sub-manifolds large degrees of entanglement results. We give analytic results for the case of two-atoms where the entanglement quantification is given through the fidelity, and Schmidt number. This gives implications for measurement protocols through Ramsey pulses, quantum simulators, and creation of spin-1 Bell states for teleportation.

Under different operating conditions, we demonstrate the emergence of electromagnetically induced transparency(EIT) which provides a platform for quantum memory, polarization conversion, and state transfer. A limitation of photonic processes is the short optical resonance lifetime, however, our system is free of this issue due to the dispersive approximation constraining the system to a decoherence free ground state manifold. As a result our EIT scheme can result in longer storage times, and more efficient state transfer as decoherence due to spontaneous emission is not the limiting factor.

DEDICATION

This work is dedicated to my parents, and to those who are not lucky enough to have this experience.

ACKNOWLEDGMENTS

Not all are lucky in this world with who they get raised by, luckily I defied the odds and was gifted into a wonderful family. My parents spent numerous hours shuttling me back and fourth between school, practice and friends houses. They pushed me to be a better thinker, athlete, and man. I owe them the world, and there isn't enough space to draw out how much I acknowledge their efforts.

It is easy as a young scientist to get caught in the draft of working fast and trying to publish before the next person. Girish Agarwal, was a large influence over the last year and really helped in developing my ability in using experiments to guide the theory, and that a good understanding of a problem cannot be done in a short amount of time. He gave many hours to answering my obvious questions, as well as, tricks and deep insights into the world that surrounds. I thank him very much, and wanted to acknowledge the amount of time he has put into me over the course of this thesis.

Finally, I would like to acknowledge my girlfriend Dallas Brister. Graduate school is filled with stress at every corner, early mornings of repeated derivations, and code not working. She has stuck by me, and helped in keeping me grounded throughout this process. I thank her very much for slogging through the mud with me.

CONTRIBUTORS AND FUNDING SOURCES

Contributors

This work was supported by a thesis (or) dissertation committee consisting of Professor Girish S. Agarwal and M.Suhail Zubairy of the Department of Physics and Professor Nevel D. Roberts of the Department of Electrical Engineering.

All of the work upheld in this thesis was conducted by the author, and supplemented by ideas from Girish S. Agarwal.

Funding Sources

Graduate study has been funded by Texas A&M through being a teaching assistant in the physics department.

NOMENCLATURE

EIT	Electromagnetically induced transparency

TABLE OF CONTENTS

Page

LIST OF FIGURES

FIGURE Page

1. INTRODUCTION

Information since first introduced by Calude Shannon has been a main institute of study in understanding how retrieving, storing, and passing information can be accomplished in the most efficient manner without loss. Quantum information addresses these questions through a different platform, one hallmarked by entanglement first introduced by Erwin Schrödinger. Quantum mechanics has advantages over classical information theory through the use of this phenomena in being able to perform classes of computations at exponentially faster rates. The photon has proven to be a strong candidate as the medium for quantum information transfer when coupled to matter. However, this idea while simple in theory, has proven to be difficult to realize due to decoherence processes, and scale to large ensembles. An emerging technique for addressing these issues is with superconducting circuits[1, 2]. The central goal of the present work is to analyze a different model, spin-1 atoms, and extend the theory of effective spin-spin interactions.

In chapter 2 we introduce the basic concepts of standard quantum optics techniques. Beginning from first principles we quantize the electromagnetic-field and derive its interaction with an ensemble of spin-$\frac{1}{2}$ atoms. Then using a technique introduced by G. Agarwal [3], we show that in a dispersive approximation the Jaynes-Cummings Hamiltonian [4] can be described by a spin-spin exchange interaction mediated by the electromagnetic field. We then discuss a recent experimental realization of this interaction from M.Norcia and J.Thompson et.al [5], where they demonstrated one-axis twisting, and the emergence of a many-body energy gap reminiscent of condensed matter systems. We conclude the chapter by showing the possible states that can result from the time evolution, and how they can be applied to measurement schemes. This not only demonstrates the power of spin theories but also introduces the mathematical formalism we extend to higher dimensional spin systems.

Motivated by recent experiments out of Stanford where spin exchange interactions were observed in a cold atomic cloud of spin-1 rubidium-87 atoms, we develop the theoretical underpinning from first principles[6, 7]. We demonstrate that beginning from the atom-light interaction the

manifold of excited states can be removed from the description through the use of time-averaging. More so, we use the uniqueness that our effective Hamiltonian theory is structured to work over many time-scales, which allows a second use of the formalism to remove the excited states. As a result we have a description solely determined by the atomic degrees of freedom mediated by intra-cavity photons. A consequence of this Hamiltonian is seen through the development of entangled states in two different settings. First, we consider the case of a fixed symmetric angular momentum manifold, where we are able to realize macroscopic superposition of states. Second, we look the opposing case when the manifolds are allowed to mix, in which case we also observe the emergence of highly entangled states which we characterize through different entanglement measures.

The final chapter focuses on electromagnetically induced transparency, first introduced by S. Harris[8]. The consequence of this resonant processes has had profound implications for quantum information science through quantum state transfer, memory, and dark state polaritons[9, 10]. We show that our model mimics the trilinear interaction similar to the one resulting from radiation pressure in optomechanics[11]. However, atomic EIT is limited by the optical excited states lifetime which eventually leads to decoherence. Optomechanical interactions occur at smaller frequencies so the dampening is not as great, and can lead to longer coherence times. However, our system is unique and EIT takes place within a decoherence free subspace, ideal for quantum information perspectives.

While atomic EIT is limited by the optical excited states lifetime, optomechanical interactions occur at lower frequencies, therefore, the resulting dampening is not decoherence inducing. The uniqueness of our system is that EIT occurs between ground states, therefore, the space is protected from decoherence, which has implications for more impactful quantum informational protocols.

2. ATOM LIGHT INTERACTION

The central theme of this thesis is to describe a new narrative of spin-1 interactions. However, it is first instructive to draw out a story that has been told several times before,which is the interaction between spin-$\frac{1}{2}$ atoms. The platform for these spin problems occur in a dispersive high-quality cavity resonator. All narratives have characters, and the first we introduce is the cavity field which is taken to be a standing wave. An ensemble of alkali-earth atoms will be the main character of study throughout this thesis. The purpose of re-illustrating the spin-$\frac{1}{2}$ story is twofold. One, it will allow us to introduce the various mathematical constructions we repeatedly use in the spin-1 case. Second, it will provide a firm base for us to refer back on when we begin describing the consequences of spin-1 interactions.

The beginning of this chapter will first discuss the physical meaning of promoting the electromagnetic field to a quantum mechanical observable through the process of canonical quantization. Section II. will be dedicated to the atom, and its interaction with the quantized field, demonstrating that the interaction is just an abstractification of an interacting harmonic oscillator. We then conclude this chapter by discussing consequences from atom-light interactions, demonstrating its utility by developing highly entangled states and their application to precision measurements.

2.1 The beauty of the Vector Potential

In classical electrodynamics the standard quantities of interest are the electric and magnetic fields[12, 13]. However, in Quantum Mechanics we are interested in observables, thus what we would like to achieve as a description of the electromagnetic field as an operator. Classicaly analytic solutions for the electric and magnetic fields is done through the use of potential functions, because in general directly determining $\vec{E}$ or $\vec{B}$ requires more difficult computations. In the absence of a local charge distribution the fields are determined through the vector potential using the relations; $\vec{E} = -\frac{\partial \vec{A}}{\partial t}$ and $\vec{B} = \nabla \times \vec{A}$. Furthermore, it is more efficient to quantize through $\vec{A}$ and then perform the derivative instead of quantizing the fields individually. Then by the Leg-

endre transformation we convert from the Lagrangian picture to the Hamiltonian which we then decompose into field operators.

In trying to develop a theory that treats the electromagnetic field as an observable, it is in fact one of an algebraic origin. Consider a map given by an exponential function, which takes compact intervals to the unit circle. This mapping is composed of elements from the Lie group $U(n)$, which is the unitary group [14]. Consider a local transformation by defining an element of the unitary group that acts on the fields, $g = e^{\phi(x)}$, where x is a spacetime coordinate. In general the Hamiltonian for a field will depend on $\psi(x)$ or $\nabla\psi$. When our g acts as a global transformation(independent of the spacetime-coordinates) then our Lagrangian will be invariant, but when g depends on the coordinates the derivative will cause an in-homogeneous term to arise. To deal with poor behavior, we introduce an affine connection which gives a precise meaning to transporting data in a consistent manner, however, removing the mathematical jargon this is just the four-vector potential $A_\mu = (A_0, \vec{A})$.

With this we can define our gauge transformation by acting on the vector potential with g.

$$\begin{aligned} A_\mu &\to gA_\mu g^{-1} + ig\partial_\mu g^{-1} \\ &\to A_\mu + \partial_\mu \phi(x) \end{aligned} \tag{2.1}$$

Before we get lost in the trees of the math, remember we are trying to motivate why we want to use the vector potential. One reason being that the connection under gauge transformations is nothing but the standard transformation in electrodynamics. The second being because it allows us to construct a new kind of derivative called the covariant derivative. The presence of this function allows us to define a curvature, which is the electromagnetic field strength tensor, $F_{\mu\nu}$. Since this is being derived from an invariant quantity of $U(1)$ then necessarily our Lagrangian will be invariant as well. The covariant derivative is defined to be, $D_\mu = \frac{\partial}{\partial_\mu} - iA_\mu$. One can show that under this definition the in-homogeneous terms will get cancelled under local gauge transformations. For a complete geometric construction we define the curvature [14]

$$\begin{aligned} F_{\mu\nu} &= i[D_\mu, D_\nu] \\ &= \partial_\mu A_\nu - \partial_\nu A_\mu \end{aligned} \tag{2.2}$$

The operation defined above is not the operator commutator we are used to but a geometrical operation known as the Lie Bracket between vector fields[14]. Mathematically, these derivatives are passing information between the algebra and the group. This mathematical interlude was provided to give a detailed explanation for why we are interested in the vector potential for quantization, mainly to ensure the Lagrangian is invariant under local gauge transformations.

2.1.1 Electromagnetic Field as Coupled Oscillators

We consider the situation where our system is not near any local charge distributions, allowing us to use the source free Maxwell Equations. We begin with the Lagrangian, which we know from construction in the previous section is gauge invariant. Proceeding with a Legendre transformation we derive the Hamiltonian through a canonically. This procedure results in a complete introduction of the first character of this story, the field. We define the kinetic energy term in the Lagrangian

$$\mathcal{L} = \frac{-1}{4\mu_0 c} F_{\mu\nu} F^{\mu\nu} \tag{2.3}$$

Which when integrated over all of space, $L = \int \mathcal{L} d^3x$ gives the total Lagrangian. Upon minimizing the action, $S = \int L d^4x$ with respect to $\dot{A_\mu}$, we find the momenta to be $\pi^\mu = \frac{\delta S}{\delta \dot{A_\mu}}$. In component form we have, $\pi^i = \frac{-E^i}{c}$ and $\pi^0 = 0$, where we used $F_{0i} = -E_i$ and $F_{ij} = \epsilon_{ijk} B_k$, [1]. Note how one of our momenta is zero, this is a result of our $U(1)$ gauge invariance from the previous section. The Legendre transformation takes our Lagrangian and moves it from configuration space to phase space, resulting in a Hamiltonian described in terms of its conjugate variables. Resulting

in the electromagnetic energy density in classical dynamics

$$H = \frac{1}{2}\int \left(\epsilon_0 E^2 + \frac{1}{\mu_0}B^2\right) d^3x \tag{2.4}$$

Our goal is now to derive operator expressions for $\vec{E}$ and $\vec{B}$ such that the Hamiltonian is now an operator function. As discussed previously we will utilize the vector potential since all other quantities can be found from it. Beginning with the wave equation

$$(\nabla^2 - \frac{1}{c^2}\frac{\partial^2}{\partial t^2})\vec{A} = 0 \tag{2.5}$$

We imagine the system placed within a large box of $V = L^3$ and apply periodic boundary conditions resulting in plane wave solutions of the form, $A(x,t) = \frac{1}{\sqrt{\epsilon_0 V}}\sum A_k(t)e^{ik\cdot r}$ where the wave vectors obey, $k_i = \frac{2\pi n_i}{L}$ and n_i is an integer. In order to arrive at 4.4 we applied a gauge fixing condition. The reason for that is because when determining the equations of motion, the conjugate momenta with respect to the scalar potential is zero. Mathematically, this means in classical phase space we can't assign all the velocities to the momenta. So the necessity of a constrained Hamiltonian must be introduced. Introducing Lagrange multipliers into the constrained Hamiltonian allows for a valid Legendre transformation. Following this process first laid out by Dirac, we find the necessary constraints lead to fixing a gauge. In the Coulomb gauge the vector potential satisfies, $\nabla \cdot \vec{A} = \frac{1}{\sqrt{\epsilon_0 V}}\sum ik \cdot A_k(t)e^{ik} = 0$ or that $k \cdot A_k = 0$. This also means that there is no longer a scalar potential, therefore, the vector potential is now a three-potential. This constraint is what allows us to consider a basis of two orthonormal vectors which will become the polarization. Plugging the solution for the vector potential into 4.5 we get

$$(\frac{\partial^2}{\partial t^2} + \omega^2)\vec{A} = 0 \tag{2.6}$$

Where we defined $\omega = ck$. The equation above is nothing but the massless Klein-Gordon Equation which can be easily solved with Fourier techniques

$$\vec{A}(x,t) = \frac{1}{\sqrt{\epsilon_0 V}} \sum_{k,s} u_{ks}(t)\vec{\epsilon_{ks}} e^{ik\cdot r} + u^*_{ks}(t)\vec{\epsilon^*_{ks}} e^{-ik\cdot r} \tag{2.7}$$

Here we defined the mode function, $u_{ks} = \alpha_{ks} e^{-i\omega t}$ and sum over wave-vectors and polarizations. Constructing the electric and magnetic field in terms of these modes as

$$\begin{aligned} \vec{E} &= \frac{i}{\sqrt{V\epsilon_0}} \sum_{ks} \omega_{ks} u_{ks} \vec{\epsilon_{ks}} e^{ik\cdot r} + C.C \\ \vec{B} &= \frac{i}{\sqrt{V\epsilon_0}} \sum_{ks} u_{ks} (\vec{k} \times \vec{\epsilon_{ks}}) e^{ik\cdot r} + C.C \end{aligned} \tag{2.8}$$

Now inserting the above expressions into the Hamiltonian

$$H = 2\sum_{ks} \omega^2 u_{ks} u^*_{ks} \tag{2.9}$$

We can re-write this equation in a more familiar form by defining functions p_{ks} and q_{ks} that satisfy the equations of motion, $\frac{\partial q_{ks}}{\partial t} = p_{ks}$ and $\frac{\partial p_{ks}}{\partial t} = -\omega^2 q_{ks}$. From this it leads, $q = u_{ks} + u^*_{ks}$ and $p = -i\omega(u_{ks} - u^*_{ks})$. Solving for the mode functions and inserting into 4.9 we recover the Hamiltonian for a classical harmonic oscillator

$$H = \frac{1}{2}\sum_{ks} (p^2_{ks} + \omega^2 q_{ks}) \tag{2.10}$$

Proceeding canonically we promote p and q to operators that satisfy, $[q_{ks}, p_{k's'}] = i\hbar\delta_{kk'}\delta_{ss'}$. Formally they are written as

$$\begin{aligned} a_{ks} &= \frac{1}{2\omega}(\omega q_{ks} + i p_{ks}) \\ a^\dagger_{ks} &= \frac{1}{2\omega}(\omega q_{ks} - i p_{ks}) \end{aligned} \tag{2.11}$$

Upon this promotion to operators we arrive at the quantized Hamiltonian for the electromagnetic field

$$H = \sum_{ks} \omega(a_{ks}^{\dagger} a_{ks} + \frac{1}{2}) \tag{2.12}$$

Along with the operator description of the fields

$$\begin{aligned} \vec{A} &= \sum_{ks} \sqrt{\frac{1}{2V\omega\epsilon_0}} a_{ks} \vec{\epsilon_{ks}} e^{i(k\cdot r - \omega t)} + H.C \\ \vec{E} &= i \sum_{ks} \sqrt{\frac{\omega}{2V\epsilon_0}} a_{ks} \vec{\epsilon_{ks}} e^{i(k\cdot r - \omega t)} + H.C \\ \vec{B} &= i \sum_{ks} \sqrt{\frac{1}{2V\omega\epsilon_0}} a_{ks} (\vec{k} \times \vec{\epsilon_{ks}}) e^{i(kr - \omega t)} + H.C \end{aligned} \tag{2.13}$$

This first section introduced the supplementary character for the story we are going to be discussing in this thesis. However, we are interested in the atom and its interaction with the field. In the following section we develop the theory of the atom, and derive the canonical model of spin-$\frac{1}{2}$ atoms. Following this we focus on developing some mathematical tools in the context of atomic cat states, and Heisenberg limited measurements, that will be used in the spin-1 theory.

2.2 The Atom and The Field

In the previous section we developed a quantum mechanical description of the supporting character in our spin-$\frac{1}{2}$ story . In this section we will introduce the main character, the atom. Furthermore, this section will be to develop the dance between the atom and the field, which we can then easily extend to the case of spin-1 atoms.

(Allow me to fade from the first person plural momentarily, and discuss the intuition for this interaction. Like the field being a harmonic oscillator, so is the atom, I imagine the atom containing a small spring locked inside oscillating at a frequency ω_a. Such that when interacting with the field it causes this little spring to either advance or slow down its oscillation. We determined the field can be described by an oscillator, which when coupled to the atom, it combines to a "big" oscillator

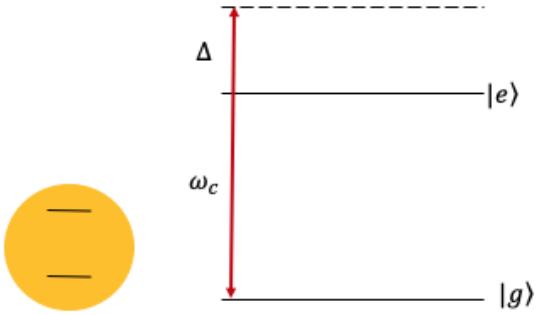

Figure 2.1: A model of a spin-$\frac{1}{2}$ atom labelled by the ground state, $|g\rangle$ separated by a transition frequency ω_a.

where the spring has been damped to a detuned frequency.)

A spin-$\frac{1}{2}$ atom is the simplest model we can conceive. The structure is composed of two energy levels, $|g\rangle$,$|e\rangle$ which spans the Hilbert space of $dim(H) = 2^{\mathcal{N}}$, where $\mathcal{N}$ is the total atom number. The quantized field causes excitations of the electron leading to transitions between these levels. Defining the zero-point energy of the atom to be in the middle of the transition, the Hamiltonian takes the form:

$$H_{atom} = \omega_a S_z \tag{2.14}$$

Where $S_z = \frac{1}{2}(|e\rangle \langle e| - |g\rangle \langle g|)$. Imagine we take the atom and place it inside a cavity motionless. Initially the cavity is taken to be in a vacuum state with the atoms cooled down so that their center of mass motion can be neglected. To this point we have taken the electric field to spatially vary in the cavity, but in practice the wavelength of the light is magnitudes larger than the size of the atom, therefore, the position dependence of the field can be neglected. This is known as the dipole approximation[15]

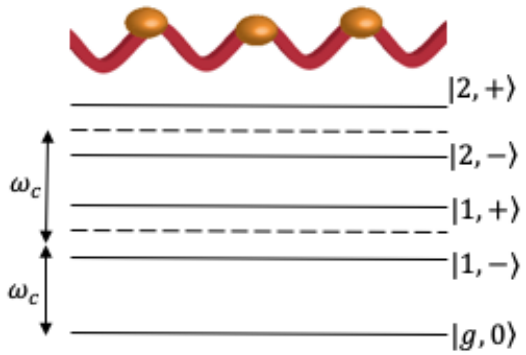

Figure 2.2: Atoms can be arranged on the node or anti-node of the cavity field, to maximize the coupling the atom is usually placed at the anti-node. The coupling induces an atom-light interaction term, $g(S_-a^\dagger + S_+a)$, which causes the the excited and ground state manifold to be dressed by the eigenstates of the Hamiltonian.

$$\begin{aligned} H_{dip} &= -\vec{d}\cdot E(\vec{r},t) \\ &= -\sqrt{\frac{\omega_c}{2\epsilon_0}}(S_- + S_+)d_{ge}(u(r)a(t) + u(r)^* a(t)^\dagger) \\ &= (S_- + S_+)(g(r)a(t) + g(r)^* a(t)^\dagger) \\ &= g(S_-a^\dagger + S_+a) \end{aligned} \tag{2.15}$$

Here $S_- = |g\rangle\langle e|$ and $S_+ = |e\rangle\langle g|$ are the raising and lowering spin operators for a single atom. We also defined the mode function from 4.9, $u(r) = \frac{e^{ik\cdot r}}{\sqrt{V}}$, such that $u(r) = 0$ on the boundary of the cavity walls and $\int |u(r)|^2 d^3r = 1$. The coupling constant, $g(r)$, arises at the location of the atom on the wave and if the wavelength is in the visible spectrum it is much larger than the atoms size, therefore, $u(r) = u(0) = 1$ so the position dependence is negligible. The reader will notice that our final form for the interaction only involves two terms instead of four. The missing terms correspond to S_-a and $S_+a^\dagger$. The physical interpretation is as follows, when the atom transitions from excited to ground state, a photon in the field is simultaneously annihilated. While the other term conveys that the atom moves from ground to excited while a photon is created. When the frequency of the atom and field are close, they correspond to non-resonant processes and as such play a minor role in the evolution when compared to the resonant processes. Thus the final step corresponds to neglecting these, hence making the rotating wave approximation[15]. We now can

present the setting of the story with the full model describing a single atom interacting with a single electromagnetic field mode, and each characters corresponding energies. This is a stripped down version of QED known as the Jaynes-Cummings model[4] which to good approximation can describe many phenomena in Quantum Optics

$$H = \omega_a S_z + g(S_- a^\dagger + S_+ a) + \omega_c a^\dagger a \tag{2.16}$$

2.2.1 Dispersive Interactions

In this section we turn to the investigation of a particular regime of the Hamiltonian derived in the previous section. We eliminate the cavity field degrees of freedom through a new method of time-averaging which is discussed in detail in the appendix. This procedure is equivalent to tracing over the field variables in the density matrix. This collective interaction has been experimentally powerful in the investigation of spin-squeezing, and quantum information[16, 5, 17].

Considering collective interactions by placing a large ensemble inside the cavity, and assuming the cloud interacts identically with the field. Making a Markov-Approximation the cloud is assumed to be dense so that the interactions take place on the same time-scale across the spatial distance of the atoms[15].

$$H = \sum_{j=1}^{N} \omega_a S_z^j + g_j(S_-^j a^\dagger + S_+^j a) + \omega_c a^\dagger a \tag{2.17}$$

Then through a unitary transformation $U = e^{iH_0 t}$ where $H_0 = H_{atom} + H_{field}$ we move into the interaction picture, where we define the atom-cavity detuning as $\Delta = \omega_c - \omega_a$

$$H_{int} = \sum_j g_j(a S_+^j e^{i\Delta t} + H.C) \tag{2.18}$$

In the dispersive regime the detuning is at a time-scale that is oscillating much faster than the scale

of the coupling, and cavity linewidth, $\Delta \gg g, \kappa$

$$\begin{aligned} H_{eff} &= \overline{-iH_{int}\int_0^t d\tau H_{int}(\tau)} \\ &= \sum_{ij} \frac{g_i g_j}{\Delta}(S_+^i S_-^j + a^\dagger a(S_+^i S_-^j - S_-^i S_+^j)) \\ &= \frac{g^2}{\Delta}(J_+ J_- + 2a^\dagger a J_z) \end{aligned} \tag{2.19}$$

When, Δ is large, $e^{i\Delta t}$, is oscillating harmonically compared to the time-scale of the dynamics of the atoms, allowing the use of the time averaging. These methods have been developed in a varying of contexts which give the same result, however, the strength of our method is in its simplicity [18, 19]. Moving from line two to three we assume the coupling to be homogeneous throughout the ensemble, and define the collective operators, $J_\pm = \sum_i^N S_\pm^i$. The final assumption we make is that the cavity is initially prepared in vacuum so that the mean photon number, $\langle 0| a^\dagger a |0\rangle = 0$. Thus our effective spin-spin interaction becomes

$$H_{eff} = \frac{g^2}{\Delta} J_+ J_- \tag{2.20}$$

Physically, this Hamiltonian is conveying the following fact about nature. When the i^{th} atom emits a photon into the cavity, the j^{th} atom absorbs it. Thus, one can imagine two spins starting anti-aligned, then when the interaction ensues, the arrows begin flip-flopping. The effective interaction is describing spin flips mediated by the electromagnetic field. This Hamiltonian is the starting point for the description of many beautiful phenomena in nature such as spin-squeezing, and non-demolition [5, 11, 20, 21].

2.3 Experimental Analysis of H_{eff}

A hallmark of Quantum optics is the study of coherence in atom-light systems, and of recent interests has been to realize quantum simulators through effective interactions. Possible realizations have been studied through phonon-mediated coupling in trapped ion systems, and direct atomic

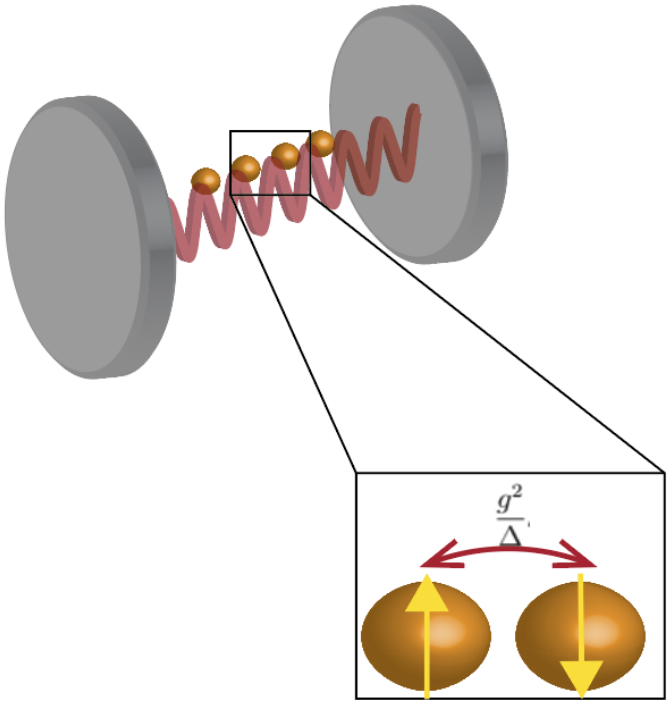

Figure 2.3: A diagrammatic description of 4.21, demonstrating how the cavity field mediates the spin-spin interaction.

collisions. A new method utilizing the effective Hamiltonian in the previous section, demonstrated tunable spin-spin exchange interactions on the clock transition of a superradiant laser [5].

The experiment is the same system we described above, where the lasing is occurring on the clock transition of Strontium-87 in the ground state manifold. Upon tuning further off resonance the cavity field can be eliminated and slaved to the atomic variables, which results in 4.21. Using the angular momentum algebra we can re-write the Hamiltonian

$$H_{eff} = \frac{g^2}{\Delta}(J^2 - J_z^2 + J_z) \tag{2.21}$$

The final term in the Hamiltonian above just is a single particle rotation and can be neglected in the large ensemble regime. The term, J_z^2 is a frequency shift which causes the states to undergo one-axis twisting. The final term, J^2 creates a many-body energy gap which prevents single particle dephasing. This similar interaction arises in the case of spin-1 atoms and it plays the role of

fixing us in a decoherence free subspace.

This model can be mapped to the Familiar Heisenberg spin-chain which in the condensed matter community displays some well known properties. One, being a global spin-precession of the collective Bloch vector, and second an opening of an energy gap. Both of these features are measured in the JILA experiment, and are a large step in developing new advances in atomic clock technology, and precision measurements.

2.4 A Quantum Zoo

The remaining part of thus chapter on spin-$\frac{1}{2}$ atoms is dedicated to applying the formalism built. First, we will introduce a zoo of states, starting with the atomic-coherent states, and their representation in the angular momentum basis, and subsequently we will demonstrate their evolution into Atomic Cat States. These states are the analog of field cat states which were first experimentally realized[13]. These highly entangled states have proved to be useful in precision measurements, which we demonstrate theoretically can reach the Heisenberg limit.

2.4.1 A new basis

This Hilbert space is a vector space determined by the Lie group $SO(3)$, whose infinitesimal generators are, σ_j where $j = 1, 2, 3$ define the Pauli-matrices. This basis is isomorphic to $\mathcal{SO}(3)$ because the commutator of the basis elements give the same description. $SO(3)$ is the group of three-dimensional rotations. Thus we can identify our Hilbert space geometrically as the sphere. Furthermore, any single spin-$\frac{1}{2}$ state can be parametrized as a point on the sphere as[22]

$$|\theta, \phi\rangle = cos\frac{\theta}{2}|g\rangle + e^{-i\phi}sin\frac{\theta}{2}|e\rangle \tag{2.22}$$

2.4.2 Dicke States

In this model we have been considering an ensemble of N two-level atoms. The most general state for the ensemble would require specifying the state for each individual atom, however, in a course-grained approximation it is adequate enough to consider the sum over all atoms. We define

the collective atomic operators as

$$J_{\pm} = \sum_{j=1}^{N} S_{\pm}^{j}$$
$$J_{z} = \sum_{j=1}^{N} S_{z}^{j} \tag{2.23}$$

Where the spin operators are in terms of Pauli matrices, $S_{\pm} = \frac{\sigma_{\pm}}{2}$. With this description if we also make the assumption the atoms are identical, then we need not to account for their spatial location since they will be interacting with the same local environments. This set of operators obeys the commutation relations,$[J_i, J_j] = i\epsilon_{ijk}J_k$, $[J_+, J_-] = 2J_z$, and $[J_z, J_{\pm}] = \pm J_{\pm}$.
A basis for the collection of two-level atoms can be assigned as

$$|\mu_1\rangle_1 |\mu_2\rangle_2 |\mu_3\rangle_3 ... |\mu_j\rangle_j ... |\mu_N\rangle_N \tag{2.24}$$

Where in the above each μ_j can take the values, $|e\rangle$ or $|g\rangle$ respectively. There are then 2^N possible states, which we define through a product state

$$|v; M\rangle = \bigotimes_{k\in v} |e\rangle_k \bigotimes_{k\notin v} |g\rangle_k \tag{2.25}$$

with the vector $\vec{v}$=$j_1, ..., j_{N/2+m}$ which denotes the number of atomic labels, and the number $N/2+m$ is the total population in the excited states, and $m = \frac{N_e - N_g}{2}$ is the atomic inversion number. These product states are eigenstates of the collective inversion operator

$$J_z |v; m\rangle = m |v; m\rangle \tag{2.26}$$

Algebraically these operators form a basis for the $su(2)$ algebra, and in representation theory, a top or bottom weight is chosen from which a ladder of eigenvalues and eigenvectors can be constructed. This "weight" is the just an eigenvalue of the "weight-space." The algebra $su(2)$ has

a finite irreducible representation, therefore, contains a highest weight state. When this state is acted on by the raising operator it has a zero-eigenvalue. Physically, this puts a restriction on the energy-eigenstates of our problem. The raising operator cannot create states above the total particle number:

$$J_+ \left| \frac{N}{2}; \frac{N}{2} \right\rangle = 0 \tag{2.27}$$

We can move up and down the ladder of inversion states by applying the raising or lowering operator. The issue is that these operators in general connect one initial product state to a whole manifold of final states which is inconvenient. To resolve this we can then introduce a new basis which is now an eigenstate of the Casimir operator of $su(2)$, which is the total collective spin, $J^2 = J_x^2 + J_y^2 + J_z^2$. We define the states as

$$\begin{aligned} J^2 \left|\lambda, j, m\right\rangle &= j(j+1) \left|\lambda, j, m\right\rangle \\ J_z \left|\lambda, j, m\right\rangle &= m \left|\lambda, j, m\right\rangle \end{aligned} \tag{2.28}$$

The allowed values of J are $\frac{N}{2}, \frac{N}{2} - 1, ..$ and orbital angular momentum, m, are bounded by $-j, j + 1, ...j$. The variable λ distinguishes between the degenerate j,m states which we will omit from this point further to follow standard convention. The ladder operators act on the Dicke states as

$$\begin{aligned} J_+ \left|j, m\right\rangle &= \sqrt{(j-m)(j+m+1)} \left|j, m+1\right\rangle \\ J_- \left|j, m\right\rangle &= \sqrt{(j+m)(j-m+1)} \left|j, m-1\right\rangle \end{aligned} \tag{2.29}$$

This algebra now only connects between single states instead of product states. We can construct these in terms of a generalization on the Bloch sphere by applying a unitary operator to the Dicke states defining the atomic coherent states[22]

$$\left|\theta, \phi\right\rangle = D(\eta) \left|j, -j\right\rangle \tag{2.30}$$

where $D(\eta) = exp(\eta J_+ - \eta^* J_-)$ and the constant $\eta = \frac{\theta}{2}e^{-i\phi}$. This unitary operator can be disentangled by using the Baker-Campbell Hausdorff formula to be

$$D(\eta) = \frac{exp(\eta J_+)}{(1+|\eta|^2)^j} \tag{2.31}$$

Upon which application to the Dicke state results in the atomic coherent state for an ensemble of atoms

$$|\theta,\phi\rangle = \sum_k^{2j} \binom{2j}{k}^{1/2} sin^k\frac{\theta}{2}cos^{2j-k}\frac{\theta}{2}e^{-ik\phi}\,|j,k-j\rangle \tag{2.32}$$

This collective expression is in terms of the basis states for the Casimir operator and J_z. These will be the starting point for our development of atomic cat states in the following section.

2.4.3 Atomic Cat States

In the previous section we developed a way to represent an ensemble of atoms in the Dicke basis, which is algebraically is related to the $su(2)$ angular momentum algebra. The initial state for the atoms is the atomic coherent state in this basis, which we will now study the consequences when evolving under non-linear evolution.

$$|\theta,\phi\rangle = \sum_k^{2j} \binom{2j}{k}^{1/2} sin^k\frac{\theta}{2}cos^{2j-k}\frac{\theta}{2}e^{-ik\phi}\,|j,k-j\rangle \tag{2.33}$$

Evolving under the Schrodinger Equation using the effective Hamiltonian 4.21

$$\begin{aligned}
|\psi(t)\rangle &= e^{-iH_{eff}t}\,|\theta,\phi\rangle \\
&= e^{-iH_{eff}t}\sum_k \binom{2j}{k}^{1/2} sin^k\frac{\theta}{2}cos^{2j-k}\frac{\theta}{2}e^{-ik\phi}\,|j,k-j\rangle \\
&= \sum_k \binom{2j}{k}^{1/2} e^{-ik\phi'} sin^k\frac{\theta}{2}cos^{2j-k}\frac{\theta}{2}e^{-i\tau(2j+t)-k^2}\,|j,k-j\rangle \\
&= \sum_k \binom{2j}{k}^{1/2} e^{-ik\phi'} sin^k\frac{\theta}{2}cos^{2j-k}\frac{\theta}{2}e^{\frac{i\pi}{m}k(k+1)}\,|j,k-j\rangle
\end{aligned} \tag{2.34}$$

Defining a new phase, $\phi^{'} = \phi + \frac{\pi}{m}(2j+2)$ and set $\tau = \frac{tg^2}{\Delta} = \frac{\pi}{m}$. To deal with the quadratic nature we check the periodicity of the unitary operator $e^{\frac{i\pi}{m}k(k+1)}$[23]. Which allows the application of Fourier decomposition by splitting the evolved state into even/odd Fourier series. First consider, $k \to k+m$

$$\begin{aligned} e^{\frac{i\pi k}{m}(k+1)} &= e^{\frac{i\pi(k+m)}{m}(k+m+1)} \\ &= (-1)^{m+1} e^{\frac{i\pi k}{m}(k+1)} \end{aligned} \tag{2.35}$$

$$\begin{aligned} e^{\frac{i\pi k^2}{m}} &= e^{\frac{i\pi}{m}(k+m)^2} \\ &= (-1)^{m} e^{\frac{i\pi k}{m}(k+1)} \end{aligned} \tag{2.36}$$

From the above results we see in the first case that our state will revive when m is an odd integer, and the second when m is an even integer. Revival is when we begin with the initial state and after a period under evolution it will return back to this state. In this problem we are beginning with an minimally uncertain state and we expect to return after a given amount of time known as the revival time which here is 2π[24]. We decompose the evolution into even and odd Fourier components as

$$\begin{aligned} e^{\frac{i\pi}{m}k(k+1)} &= \sum_{q}^{m-1} f_q^{(o)} e^{\frac{2\pi i q}{m}k} \\ e^{\frac{i\pi}{m}k^2} &= \sum_{q}^{m-1} f_q^{(e)} e^{\frac{2\pi i q}{m}k} \end{aligned} \tag{2.37}$$

Where f_q^o, f_q^e are even and odd coefficients respectively as

$$\begin{aligned} f_q^{(o)} &= \frac{1}{m}\sum_{k}^{m-1} e^{\frac{-2\pi i q}{m}k} e^{\frac{i\pi}{m}k(k+1)} \\ f_q^{(e)} &= \frac{1}{m}\sum_{k}^{m-1} e^{\frac{-2\pi i q}{m}k} e^{\frac{i\pi}{m}k^2} \end{aligned} \tag{2.38}$$

From a mathematical perspective this is useful because we took a result that was quadratic in the eigen-energies and linearized them through a decomposition. But, this is an insightful result from a physical perspective as well. Imagine you want to run an experiment and you are interested in determining a particular state that is a result of some non-linear evolution. Provided it is periodic you can determine the collapse and revival times which allows the experimentalist to probe time their dynamics systematically. Beginning from an atomic coherent state the evolution has resulted in even and odd coherent states that are out of phase with one another.

$$\begin{aligned} |\psi(t)\rangle_{odd} &= \sum_{q}^{m-1} f_q^{(o)} |\theta, \phi + \frac{\pi}{m}(2j + 2 - 2q) > \\ |\psi(t)\rangle_{even} &= \sum_{q}^{m-1} f_q^{(e)} |\theta, \phi + \frac{\pi}{m}(2j + 1 - 2q) > \end{aligned} \tag{2.39}$$

A method to see the cat states arise under time evolution is to look at the diagonal components of the density matrix, which represent the population statistics of the atoms. To determine this we use a quasi-probability distribution [25, 22], known as the $\mathcal{Q}$-function. There are several other functions of merit to quantify the dynamics of the state such as the P-representation or Wigner function. The problem with the P-representation is that this function need not always exist, on the other hand the Wigner function, while it always exists, it strays away from the meaning of probability distribution as it can become negative. Also, since our goal is to look at systems of higher spin the $\mathcal{Q}$-function is easy to calculate numerically, while the Wigner function depends on the algebraic properties of the group because it ultimately is an integral over the group volume(Haar measure), which are notoriously difficult to calculate for higher $\mathcal{SU}(N)$ groups[26, 27, 28]. The $\mathcal{Q}$-function in terms of the angles defining the atomic coherent state is defined as

$$\mathcal{Q} = \frac{2j+1}{4\pi} \langle \theta, \phi | \, \rho \, | \theta, \phi \rangle \tag{2.40}$$

Here ρ is the density matrix defined to be, $\rho = |\psi(t)\rangle \langle \psi(t)|$. In order to see the how the state evolves we calculate the density matrix at various times on the interval, $[0, 2\pi]$ and plot the $\mathcal{Q}$-

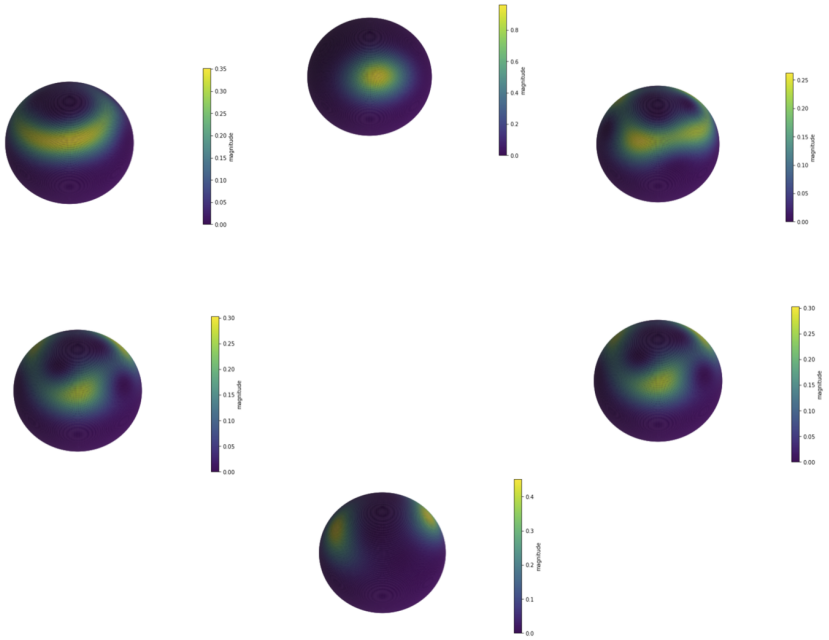

Figure 2.4: Q-function from simulation time-evolution of atomic-coherent states with the effective Hamiltonian. The top position is the initial atomic coherent state in $\left|-\frac{\pi}{2}, \frac{\pi}{2}\right\rangle$. The time-evolution is seen by moving clockwise, at which the bottom position we see two distinct distributions which represent the coherent superposition of states out of phase. At $t = \frac{\tau\Delta}{mg^2} = 2\pi$ we recover the initial state showing the periodicity.

function on the Bloch sphere (Fig 2.4). In the diagram we see that initially the ensemble starts localized, and upon time evolution the distribution is slowly separates until we see two well localized distributions. At this point the state is in a superposition of atomic coherent states, known as an atomic cat state. Continuing the evolution at $t = 2\pi$ we have a complete revival to the initial state.

Several theoretical schemes have been put forward to generate these states and have recently even been verified an experimental setting[29, 30], and now that we have mathematically demonstrated their possibility of existence, we would like to discuss what makes them difficult to detect. The evolution time is defined as $t = \frac{\pi\Delta}{mg^2}$. If one wants to experimentally create these states, we need to generate coherence between the atoms as fast as possible in order to prevent rapid decoherence due to heating and atomic collisions. To achieve this we need our time to be small which implies that g must be large, however, this parameter is influenced by experimental tech-

nicalities and it wasn't until superconducting cavities were utilized did this regime become more accessible[31, 32].

2.4.4 How precise can we be?

The final portion of this chapter is dedicated to an application of these states, and how powerful they can be in non-demolition schemes. Imagine we want to create a new device, that requires precise measurements of particular quantities such as time. Furthermore, we want an atomic clock that gives measurements proportional to $1/\mathcal{N}$ where $\mathcal{N}$ is the total number of atoms in the cavity. Achieving this value is known as the Heisenberg limit which is an upper bound on how precise a measurement can be as a result of the energy-time uncertainty principle. In this final section we demonstrate how cat states result in measurements of an arbitrary phase of an interferometer that can reach this bound. The experiment we are considering is shown in the figure. Consider input light through a beam-splitter where we interested in measuring a random phase. We consider the atoms to be initialized in a product state

$$|\psi(0)\rangle = \prod_{j=1}^{N} |g\rangle_j \tag{2.41}$$

To generate the atomic cat states we apply a non-linear rotation on $|\psi(0)\rangle$

$$|\psi(t)\rangle = e^{\frac{i\pi}{2}J_x^2} |\psi(0)\rangle \tag{2.42}$$

Utilizing our mathematical tricks from the previous sections we want to linearize this operation. Writing, $J_x = e^{\frac{i\pi}{2}J_y} J_z e^{\frac{-i\pi}{2}J_y}$, we see that the eigenvalues of this operator are going to be integers proportional to J_z. Therefore, J_x^2 will be proportional k^2 where k is an integer, which from the previous section is periodic in an integer m

$$e^{\frac{i\pi}{m}J_x^2} = \sum_{q}^{m-1} f_q^{(e)} e^{\frac{2\pi i q}{m}J_x} \tag{2.43}$$

We now specify to the case of m=2 and derive analytic solutions

$$\begin{aligned} e^{\frac{i\pi}{2}J_x^2}\left|\psi(0)\right\rangle &= \sum_q^{m-1} f_q^{(E)} e^{\frac{2\pi i q}{m}J_x}\left|\psi(0)\right\rangle \\ &= \frac{1}{\sqrt{2}}e^{\frac{i\pi}{4}}\left|ggg..\right\rangle + \frac{1}{\sqrt{2}}e^{\frac{-i\pi}{4}}e^{i\pi J_x}\left|ggg..\right\rangle \\ &= \frac{1}{\sqrt{2}}e^{\frac{i\pi}{4}}(\left|ggg..\right\rangle + (i)^{N-1}\left|ee..\right\rangle) \end{aligned} \tag{2.44}$$

We saw in deriving the Dicke States we can move between the computational and angular momentum basis by unitary operators. The cat states derived in the previous rotate into the states above under $e^{\frac{-i\pi J_y}{2}}$. Physically, this means we can create another state to add to our quantum zoo, known as a GHZ. The GHZ state is just the atomic cat state in a rotated basis, where in this problem the angles are $\theta = \pi/2$ and $\phi = -\pi/2$[25]. Next we perform the step that introduces the phase to be measured

$$e^{i\phi J_z}e^{\frac{i\pi}{2}J_x^2}|\psi(0)> = \frac{1}{\sqrt{2}}e^{\frac{i\pi}{4}}(e^{\frac{-iN}{2}\phi}|gggg...> + (i)^{N-1}e^{\frac{iN}{2}\phi}|eee...>) \tag{2.45}$$

Where $e^{i\phi J_z} = e^{i\phi\sum\sigma_z} = \prod e^{i\phi\sigma_z}$. To complete the measurement scheme we apply the inverse non-linear transformation which amounts to i going to $-i$.

$$\begin{aligned} \left|\psi_{out}\right\rangle &= e^{\frac{-i\pi}{2}J_x^2}e^{i\phi J_z}e^{\frac{i\pi}{2}J_x^2}\left|\psi(0)\right\rangle \\ &= \cos\left(\frac{N}{2}\phi\right)\left|gg..\right\rangle + i^N\sin\left(\frac{N}{2}\phi\right)\left|ee..\right\rangle \end{aligned} \tag{2.46}$$

To characterize the precision measurement we need to determine the sensitivity of our phase by applying the error-propagation formula, by first determining the variance of the collective inversion operator

$$\begin{aligned} \left\langle\psi_{out}\right| J_z \left|\psi_{out}\right\rangle &= -\frac{N}{2}\cos N\phi \\ \Delta J_z &= \sqrt{\left\langle\psi_{out}\right| J_z^2 \left|\psi_{out}\right\rangle - \left\langle\psi_{out}\right| J_z \left|\psi_{out}\right\rangle^2} \end{aligned} \tag{2.47}$$

With the above result we find the sensitivity to be

$$\begin{aligned}\Delta\phi &= \sqrt{\frac{\Delta J_z}{(\frac{\partial\langle\psi_{out}|J_z|\psi_{out}\rangle}{\partial\phi})^2}} \\ &= \frac{1}{N}\end{aligned} \tag{2.48}$$

Furthermore, there highly entangled states played a major role in this scheme reaching the upper bound in precision measurement. This theoretical work has recently been carried out in a variety of experiments[33, 34, 35, 36].

This chapter primarily was to introduce the simplest atom-light interaction; an ensemble of spin-$\frac{1}{2}$ atoms interacting with a single cavity field. We then derived atomic cat states through the evolution of an effective spin-spin interaction. These then proved to be valuable in a particular measurement scheme where we found that in a beam-splitter we can reach the Heisenberg limit. The remainder of this thesis is focused on spin-1 atoms, and its interaction with the electromagnetic field. We focus on a first principle derivation of the effective spin-spin interaction and demonstrate how we can realize spin-1 cat states in a symmetric subspace, and how we can map the physics to a optomechanical interaction and realize electromagnetically-induced transparency.

3.1 Spin-1 Interactions

A central goal of quantum information is to study coherence and its consequences. Applications for systems demonstrating stronger coherence include macroscopic states, quantum memory, and state transfer[37, 9, 10]. A central problem with the system we described in the previous chapter is spontaneous emission, while experimentally the dynamics can occur in a ground state manifold, there is still heating from the transitions. Heating leads to rapid decoherence, which prevents the creation of long lived states for the applications above. In this chapter we theoretically describe a platform that is robust to decoherence due to the absence of spontaneous emission in the ground state manifold. First, we give a description of the atom-light interaction for spin-1 atoms and a single cavity mode through the dipole Hamiltonian. We show that in the dispersive regime we can adiabatically eliminate the excited state leaving a Hamiltonian described completely by the ground states. We end the chapter by changing from the computational basis to a collective spin description.

3.1.1 Spin-1 Model

The model we are going to derive is to represent an ensemble of spin-1 atoms interacting with a quantized cavity mode. The cavity field is taken to be quantized along the x-direction with polarizations in the y direction denoted as horizontal and z direction as the vertical. The starting point is the quantized electromagnetic field

$$\begin{aligned}\vec{E}(x,t) &= i\sqrt{\frac{\hbar\omega_c}{2\epsilon_o}}\sum_{\sigma}\left(a_\sigma\vec{\epsilon_\sigma}u(x) - a_\sigma^\dagger\vec{\epsilon_\sigma^*}u(x)^*\right) \\ &= i\sqrt{\frac{\hbar\omega_c}{2\epsilon_o}}\left((a_y\vec{\epsilon_y} + a_z\vec{\epsilon_z})u(x) - (a_y^\dagger\vec{\epsilon_y^*} + a_z^\dagger\vec{\epsilon_z^*})u(x)^*\right)\end{aligned} \tag{3.1}$$

Here the mode functions are defined as, $u(x) = \frac{e^{ik\cdot x}}{\sqrt{V}}$ with the normalization $\int_0^L |u(x)|^2 d^3x = 1$. Our first approximation to the theory is that for an atomic system $k \cdot x$ is going to be small number

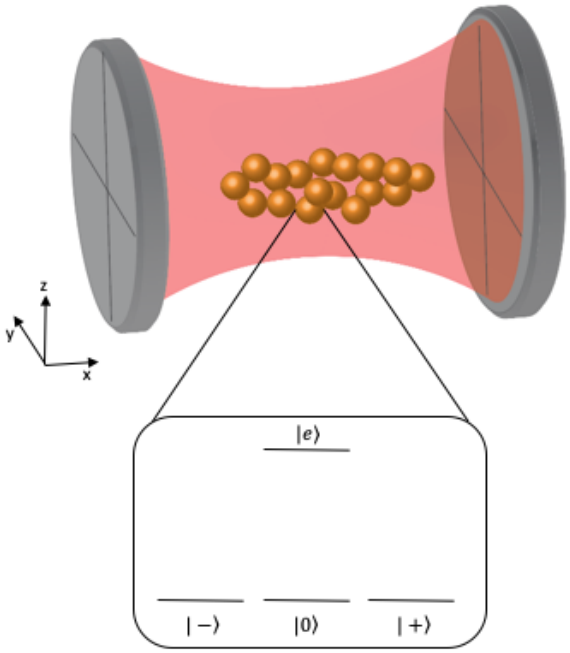

Figure 3.1: The cavity field(red) is taken along the x-direction, with the atoms(orange) places in the cavity. We model an atom as an excited and ground state manifold. The excited state is taken to be $F = 0$, $m_f = 0$ angular momentum and ground state $F = 1$, $m_f = -1, 0, +1$.

because $k \cdot x = \frac{2\pi}{\lambda} a_o$ where λ is the wavelength of the cavity field and a_o is the Bohr Radius[15]. Provided the light field is in the visible spectrum, the wavelength is much larger than the size of the atom. This allows us to set $u(x) = u(0) = 1$ which is the electric-dipole approximation. We now construct the dipole operator by applying the identity to both sides of $\hat{d}$ and using the fact that transitions within the ground state manifold are dipole forbidden

$$\vec{d} = \langle e|\, \vec{d}\, |0\rangle\, |e\rangle\, \langle 0| + \langle e|\, \vec{d}\, |+\rangle\, |e\rangle\, \langle +| + \langle e|\, \vec{d}\, |-\rangle\, |e\rangle\, \langle -| + H.C \tag{3.2}$$

The dipole-interaction is then taken to be

$$H_{dip} = -q\vec{r} \cdot \vec{E}(x,t) \tag{3.3}$$

Using the definition of our above operators for the field and dipole

$$H_{dip} = g_0 \left|e\right\rangle \left\langle 0\right| a_z + g_0^* \left|0\right\rangle \left\langle e\right| a_z^\dagger + g_+ \left|e\right\rangle \left\langle +\right| a_y + g_+^* \left|+\right\rangle \left\langle e\right| a_y^\dagger + g_- \left|e\right\rangle \left\langle -\right| a_y + g_-^* \left|-\right\rangle \left\langle e\right| a_y^\dagger \tag{3.4}$$

In deriving the Hamiltonian above we considered the model atom to be rubidium-87 where the excited state manifold consisting of a single level is given by $F = 0$ and $m_f = 0$[38]. The ground state manifold is then, $F = 1$ and respectively all orbital angular quantum numbers $m_f = -1, 0, +1$, see 3.1. Then using our defined coordinate system the only non-zero matrix elements are given by; $\langle e| (z \cdot \vec{\epsilon_z}) |0\rangle$, $\langle e| (y \cdot \vec{\epsilon_y}) |+\rangle$, $\langle e| (y \cdot \vec{\epsilon_y}) |-\rangle$, along with their complex conjugates. The effective couplings are defined as, $g_f = q\sqrt{\frac{\hbar\omega_c}{2V\epsilon_o}}$ from which it follows: $g_o = -ig_f \langle e| (z \cdot \vec{\epsilon_z}) |0\rangle$, $g_+ = -ig_f \langle e| (y \cdot \vec{\epsilon_y}) |+\rangle$, and $g_- = -ig_f \langle e| (y \cdot \vec{\epsilon_y}) |-\rangle$. In arriving at Eq 3.4 we made one other approximation which are the terms that go as, $|e\rangle \langle 0| a_z^\dagger$ and $|0\rangle \langle e| a_z$ along with all permutations of the states. If the frequency of the field and the atom are nearly resonant these terms will correspond to non-resonant terms and thus will play little role in the evolution of the system, and so we can neglect them[15]. With the atom-light Hamiltonian we now write down the rest of the system, for the field and atomic energy levels

$$\begin{aligned} H_{field} &= \omega_c (a_y^\dagger a_y + a_z^\dagger a_z) \\ H_{atom} &= \sum_i \omega_i \left|i\right\rangle \left\langle i\right| \end{aligned} \tag{3.5}$$

Here ω_i is the atomic frequency and i indicates the level, for example $|e\rangle \langle e|$, not the atom number, and ω_c is the cavity frequency. For the remainder of this chapter we will consider an ensemble of atoms in the cavity unless stated otherwise. The atomic cloud is taken to be dense so that we can assume a Markov approximation for how the atoms interact with the field mode. We then sum over all atoms and define, $S_{ij} = |i\rangle \langle j|$ for convenience. It is important to point out that

these are not collective operators

$$
\begin{aligned}
H_{field} &= \omega_c(a_y^\dagger a_y + a_z^\dagger a_z) \\
H_{atom} &= \sum_i S_{jj}^i \omega_j \\
H_{dip} &= \sum_i g_0 S_{e0}^i a_z + g_0^* S_{0e}^i a_z^\dagger + g_+ S_{e+}^i a_y + g_+^* S_{+e}^i a_y^\dagger + g_- S_{e-}^i a_y + g_-^* S_{-e}^i a_y^\dagger
\end{aligned}
\tag{3.6}
$$

It is now most convenient to work in the interaction picture by applying a transformation using the free Hamiltonian.

$$
H_{int} = \sum_i g_0 S_{e0}^i a_z e^{i\Delta t} + g_0^* S_{0e}^i a_z^\dagger e^{-i\Delta t} + g_+ S_{e+}^i a_y e^{i\Delta t} + = g_+^* S_{+e}^i a_y^\dagger e^{-i\Delta t} + g_- S_{e-}^i a_y e^{i\Delta t} + g_-^* S_{-e}^i a_y^\dagger e^{-i\Delta t}
\tag{3.7}
$$

In 4.7 $\Delta = \omega_i - \omega_c$ is the atom-cavity detuning. In deriving the above equation we used that an operator transforms as, $O(t) = e^{iHt} O e^{-iHt}$ and that the commutation relation between the pseudo-spin operators are $[S_{ij}, S_{kl}] = \delta_{kj} S_{il} - \delta_{il} S_{kj}$. We now make a further approximation to the theory which is when the detuning is the dominating time-scale, $\Delta \gg g_i, \kappa$ where κ is the cavity line-width. In this dispersive approximation the exponential oscillate harmonically, allowing the

application of our time averaging procedure, described in Appendix A.

$$
\begin{aligned}
H_{eff} &= H_{spon} + H_{stark} + H_{Raman} + H_{coupling} \\
H_{spon} &= \sum_{ij} \frac{g_+ g_+^*}{\Delta} S^i_{e+} S^j_{+e} + \frac{g_- g_-^*}{\Delta} S^i_{e-} S^j_{-e} + \frac{g_- g_+^*}{\Delta} S^i_{e+} S^j_{-e} + \frac{g_+ g_-^*}{\Delta} S^i_{e-} S^j_{+e} + \frac{g_0 g_0^*}{\Delta} S^i_{e0} S^j_{0e} \\
H_{stark} &= \sum_{ij} \frac{g_+ g_+^*}{\Delta} (S^i_{e+} S^j_{+e} - S^i_{+e} S^j_{e+}) a_y^\dagger a_y + \frac{g_- g_-^*}{\Delta} (S^i_{e-} S^j_{-e} - S^i_{-e} S^j_{e-}) a_y^\dagger a_y + \frac{g_0 g_0^*}{\Delta} (S^i_{e0} S^j_{0e} - S^i_{0e} S^j_{e0}) a_z^\dagger a_z \\
H_{Raman} &= \sum_{ij} -\frac{g_- g_+^*}{\Delta} S^i_{+e} S^j_{e-} - \frac{g_+ g_-^*}{\Delta} S^i_{-e} S^j_{e+} a_y^\dagger a_y + \frac{g_+ g_-^*}{\Delta} S^i_{e+} S^j_{-e} + \frac{g_- g_+^*}{\Delta} S^i_{e-} S^j_{+e} a_y^\dagger a_y \\
H_{coupling} &= \sum_{ij} \frac{g_0 g_+^*}{\Delta} S^i_{e0} S^j_{+e} a_y^\dagger a_z - \frac{g_+ g_0^*}{\Delta} S^i_{0e} S^j_{e+} a_z^\dagger a_y + \frac{g_0 g_-^*}{\Delta} S^i_{e0} S^j_{-e} a_y^\dagger a_z - \frac{g_- g_0^*}{\Delta} S^i_{0e} S^j_{e-} a_z^\dagger a_y \\
&\quad + \frac{g_+ g_0^*}{\Delta} S^i_{e+} S^j_{0e} a_z^\dagger a_y - \frac{g_0 g_+^*}{\Delta} S^i_{+e} S^j_{e0} a_y^\dagger a_z + \frac{g_- g_0^*}{\Delta} S^i_{e-} S^j_{0e} a_z^\dagger a_y - \frac{g_0 g_-^*}{\Delta} S^i_{-e} S^j_{e0} a_y^\dagger a_z
\end{aligned}
\tag{3.8}
$$

The interaction between spin-1 atoms is more complicated than the Jaynes-Cummings effective theory because higher multipole moments from the electromagnetic field are manifesting. Later in the chapter, we show these are coming through as second rank tensors in the atomic field operators. We can simplify by expanding the sum into $i = j$ and $i \neq j$, the latter term vanishes in all terms above except for the spontaneous emission

$$
\begin{aligned}
H_{spon} &= \sum_{i \neq j} \frac{2g^2}{\Delta} S^i_{e0} S^j_{0e} + \frac{g^2}{\Delta} S^i_{e+} S^j_{+e} + \frac{g^2}{\Delta} S^i_{e-} S^j_{-e} - \frac{g^2}{\Delta} S^i_{e-} S^j_{+e} - \frac{g^2}{\Delta} S^i_{e+} S^j_{-e} \\
&\quad + \sum_i \frac{2g^2}{\Delta} S^i_{ee} + \frac{g^2}{\Delta} S^i_{ee} + \frac{g^2}{\Delta} S^i_{ee} \\
H_{stark} &= \sum_i \frac{g^2}{\Delta} (S^i_{ee} - S^i_{++}) a_y^\dagger a_y + \sum_i \frac{g^2}{\Delta} (S^i_{ee} - S^i_{--}) a_y^\dagger a_y + \sum_i \frac{g_0^2}{\Delta} (S^i_{ee} - S^i_{00}) a_z^\dagger a_z \\
H_{Raman} &= \sum_i \frac{g^2}{\Delta} (S^i_{+-} + S^i_{-+}) a_y^\dagger a_y \\
H_{coupling} &= \sum_i \frac{i\sqrt{2} g^2}{\Delta} (S^i_{+0} - S^i_{-0}) a_y^\dagger a_z + \frac{i\sqrt{2} g^2}{\Delta} (S^i_{0-} - S^i_{0+}) a_z^\dagger a_y
\end{aligned}
\tag{3.9}
$$

In chapter 1 we found that it was easier to deal with dynamics when working in the collective angular momentum basis. Therefore, we determine a transformation from the computational to

angular momentum basis in the following. The spin-1 algebra will be discussed in more depth in later chapters, so we just quote the form of the operators here. $F_z^j = |+\rangle\langle+|_j - |-\rangle\langle-|_j$ and $F_+^j = \sqrt{2}(|+\rangle\langle 0| + |0\rangle\langle -|)_j$, $F_-^j = \sqrt{2}(|-\rangle\langle 0| + |0\rangle\langle +|)_j$. Using non-linear combinations of the operators we can construct the S_{ij} in terms of these. For example the states, $S_{0+}^j = \frac{F_-^j F_z^j}{\sqrt{2}}$, $S_{0-}^j = \frac{-F_+^j F_z^j}{\sqrt{2}}$. We then define the collective operators, $F = \sum_{j=1}^N F^j$. We then make an approximation to the excited states, since we are working in the regime, $\Delta/g >> \kappa$, the probability that the atom reaches the excited state manifold is negligible,therefore, we neglect terms with $|e\rangle\langle e|$

$$\begin{aligned} H_{stark} &= -\frac{g^2}{\Delta}F_z^2 a_y^\dagger a_y - \frac{2g^2}{\Delta}(1-F_z^2)a_z^\dagger a_z \\ H_{Raman} &= \frac{g^2}{\Delta}(F_x^2 - F_y^2)a_y^\dagger a_y \\ H_{coupling} &= \frac{-g^2}{\Delta}((a_z^\dagger a_y + a_y^\dagger a_z)F_y + i(F_x F_z + F_z F_x)(a_z^\dagger a_y - a_y^\dagger a_z)) \end{aligned} \tag{3.10}$$

Before we proceed in adiabatically eliminating the cavity modes, and discussing a more physical picture. Lets discuss why the Hamiltonian takes the form that it does. In the above equations, the Hamiltonian is constructed of three types of terms; scalar, vector, and tensor. We will discuss each of these in succession and their relevance to experimental situations.

First, the scalar term arising in the Stark shift Hamiltonian. The Hilbert space structure is given by, $Id \otimes a_y^\dagger a_y$. Theoretically, and experimentally we are interested in the observables related to the atomic degrees of freedom, and since this term is proportional to the identity on the atomic Hilbert Space and can be eliminated by tuning a probe to the magic-zero or tune-out wavelength[39, 40, 41].

Second, the vectorial term which is linear in the atomic operators admits a nice interpretation in a classical electrodynamics. Noticed first by Faraday, when a medium subjected to light and a magnetic field it causes the plane of polarization to undergo a rotation[42]. This is what the vectorial term is telling us, the field propagating in the x-direction undergoes a rotation by the interaction with the atoms in the cavity. In optics this interaction has played a fundamental role in non-demolition of quantum spin systems[43, 44] and will be our main course of study in the

remaining portion of this thesis.

Finally, the tensor terms which contains all the quadratic operators. While vector terms was rotating the circular modes of the field, these are doing the same except now to the elliptical modes arising from the quadrapole moments of the field. Theoretically these terms are hard to deal with if we want to develop an only spin degree system. It turns out that experimentally the procedure of dynamic decoupling[21] for pulsed measurement schemes will eliminate this term. It was demonstrated that this term in general vanishes if the probe field and externa1 magnetic field are at $ArcTan(\sqrt{2})$ to one-another[45, 46]. Furthermore, for the remainder of this thesis we will focus on the vector term, and how we can realize spin-spin interaction from it.

4. PHOTON MEDIATED INTERACTIONS BETWEEN SPIN-1 ATOMS

In the previous chapters we dealt purely with the Hamiltonian describing the atom and the light, we found that the physics of this interaction can be mapped classically to the Faraday Effect, along with higher quadrupole moments. Using experimental techniques for the type of problem we are interested in, we neglect higher order corrections and purely focus on the vector term. In this chapter we are going to describe this interaction in perturbation theory by moving into the dispersive regime, allowing us to apply the method of time-averaging. Through adiabatic elimination of the fields we derive a Hamiltonian describing spin flips between spin-1 atoms, which will resemble the physics of what we did in Chapter 1. With this model we will investigate certain consequences. First, we will investigate the preparation of highly entangled states when working in a fixed angular momentum manifold. Next, we will look into the story of when we allow angular momentum mixing, and finally we discuss how one may develop electromagnetically induced transparency, which mimics interactions in optomechanical systems.

4.1 Spin-1 Model

An outstanding goal of physics is to be able to encode information in highly entangled states with long coherence times. However, entanglement is a non-local process while the interactions are necessarily local which in turn puts a restriction on the allowable states. In this section we derive an effective non-local interaction by eliminating the cavity modes, resulting in a pure spin degree of freedom system. These sort of interaction are only recently being engineered in experimental setting first used for quantum metrology on atomic clock transitions[5, 20], and processes analogous to spin-mixing in Bose-Einstein Condensates[47, 48]. We find that these states are particularly useful for replicating interactions similarly found in optomechanical settings.

4.2 Adiabatic Elimination of Cavity modes

The scheme for generating spin-spin interactions is given in the 4.1. There is a Fabry-Perot cavity supporting an electromagnetic field propagating in the x-direction. We then consider a

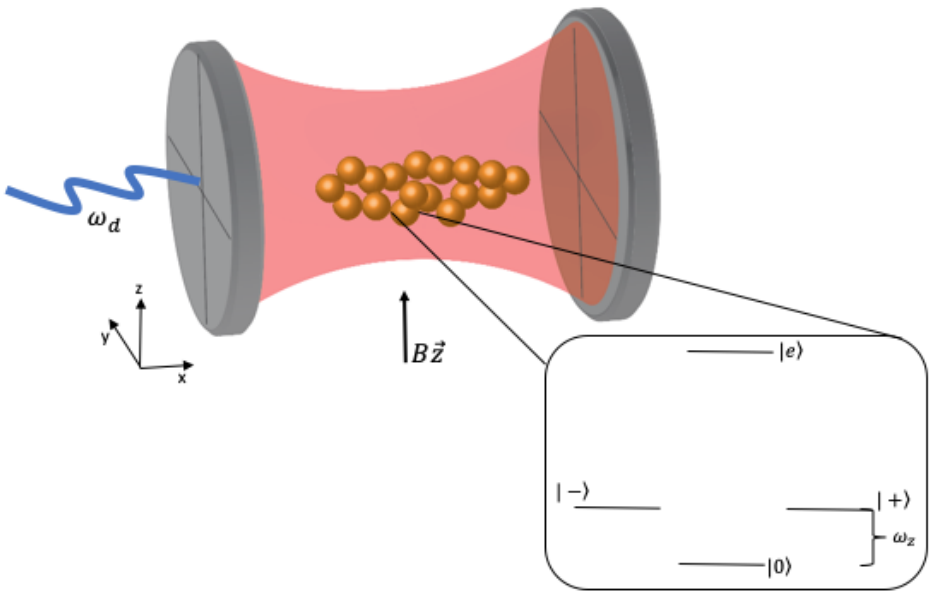

Figure 4.1: Depiction of the system being studied. A dispersive high quality resonator being driven by a control field polarized in y. An applied static magnetic field in z causes the degenerate ground states to split by an energy gap of the Zeeman frequency.

static magnetic field applied perpendicular to the cavity axis in z. The Raman processes arise from a strong control field applied with polarization in the y-direction. This results in the Hamiltonian given by

$$\begin{aligned} H_{AL} &= \frac{-g^2}{\Delta}((a_z^\dagger a_y + a_y^\dagger a_z)F_y \\ H_B &= \omega_z F_z \\ H_d &= i\epsilon_y(a_y^\dagger e^{-i\omega_d t} - a_y e^{i\omega_d t}) \\ H_f &= \omega_c(a_y^\dagger a_y + a_z^\dagger a_z) \end{aligned} \tag{4.1}$$

Where the angular velocity of the magnetic field is, $\omega_z = -\gamma B$ where γ is the gyromagnetic ratio for the atom, and finally $\epsilon_y = \sqrt{\frac{2\kappa\mathcal{P}}{\omega_d}}$. In the previous definition, $\mathcal{P}$ is the power of the drive field, κ is the linewidth of the field, and ω_d is the drive frequency. We take the drive field to be strong so that we can approximate it by a classical field in steady state. To determine the approximate steady

state value we derive the Heisenberg equation of motion and use the ansatz, $a_y = \alpha_y e^{-i\omega_d t}$

$$\begin{aligned}\frac{da_y}{dt} &= i[H, a_y] + \kappa([a_y^\dagger, a_y]a_y + a_y^\dagger[a_y, a_y]) \\ &= (-\kappa - i\omega_c)a_y + \epsilon_y e^{-i\omega_d t}\end{aligned} \tag{4.2}$$

Which by setting to zero with the ansatz we find $\alpha_y = \frac{\epsilon_y}{\kappa + i(\omega_d - \omega_c)}$. Going into the interaction picture and defining the cavity-drive detuning, $\delta = \omega_d - \omega_c$, our Hamiltonian becomes

$$H = \frac{\Omega}{2i}(a_z^\dagger \alpha_y F_+ e^{-i(\delta+\omega_z)t} - a_z \alpha_y^* F_- e^{i(\delta+\omega_z)t} - a_z^\dagger \alpha_y F_- e^{-i(\delta-\omega_z)t} + a_z \alpha_y^* F_+ e^{i(\delta-\omega_z)t}) \tag{4.3}$$

The generation of coherent interactions is a result of the drive field being off Raman resonance. Tuning the drive field to δ results in the two photon Raman resonance detuning, $\Delta_+ = \delta + \omega_z$ and $\Delta_- = \delta - \omega_z$. When on two-photon resonance we expect the system to be in a superradiant regime, but as the frequency of the fields get increased the decay gets suppressed leading to coherent dynamics in the ground state manifold[6]. Hencefourth, the Hamiltonian takes the form

$$H = \frac{\Omega}{2i}(a_z^\dagger \alpha_y F_+ e^{-i\Delta_+ t} - a_z \alpha_y^* F_- e^{i\Delta_+ t} - a_z^\dagger \alpha_y F_- e^{-i\Delta_- t} + a_z \alpha_y^* F_+ e^{i\Delta_- t}) \tag{4.4}$$

We are again faced with the situation where we have fast oscillating exponential when $\Delta_\pm \gg \epsilon_y$, allowing us to apply the time-averaging procedure[3]. Upon doing the calculation, we get terms that appear as, $e^{i(\Delta_+ \pm \Delta_-)t}$. We cannot just assume that these terms will average to zero based off of previous approximation to eliminate the excited states. For the equation below to be valid, the systems need to be far off of two-photon Raman resonance. The reason for this is that as we approach the resonance condition the system induces superradiant decay. To achieve the former we make a second time-scale approximation and require, $|\Delta_+ \pm \Delta_-| \gg |\Omega \alpha_y|$. Provided, this

holds the exponential's can be taken to be zero, and the resulting Hamiltonian is

$$H = \left(\frac{\Omega}{2i}\right)^2 \left(\frac{|\alpha_y|^2}{\Delta_+} a_z^\dagger a_z F_+ F_- - \frac{|\alpha_y|^2}{\Delta_+} a_z a_z^\dagger F_- F_+ + \frac{|\alpha_y|^2}{\Delta_-} a_z^\dagger a_z F_- F_+ - \frac{|\alpha_y|^2}{\Delta_-} a_z a_z^\dagger F_+ F_- \right) \tag{4.5}$$

To complete the derivation we make a final approximation to eliminate the fields. If a_z is initially in vacuum, then, $\langle 0| a_z^\dagger a_z |0\rangle = 0$ and $\langle 0| a_z a_z^\dagger |0\rangle = 1$ resulting in

$$H = \frac{|\Omega \epsilon_y/2|^2}{\kappa^2 + \delta^2} \left(\frac{F_+ F_-}{\Delta_-} + \frac{F_- F_+}{\Delta_+} \right) \tag{4.6}$$

This pairwise interaction is interesting because the coupling is controlled by the drive field amplitude, where the sign of the interaction can be varied depending on the two-photon detuning. More so, upon a transformation this effective Hamiltonian can be expressed as a spin-1 Heisenberg XY with a transverse magnetic field in z. The sign of the interaction then determines if it ferromagnetic or anti-ferromagnetic, which is demonstrated in the experiment by E.Davis et.al where they saw the magnetization flip between ferromagnetic and anti-ferromagnetic order as the cavity-drive detuning was swept through resonance. The spin-flip process is seen by hopping between the sites mediated by an intra-cavity photon. Interestingly, in the experiment [6] they found that the interactions feel a time-dependent spatial-gradient on the cloud on the time-scale of the spin exchange. The atoms probabilistically were hopping towards the left edge of the cloud, the reason for this is that coupling is not homogeneous. In the cavity the ensemble is initially displaced from cavity center causing the excitations to "prefer" a direction to hop initially.

4.2.1 Symmetric Dicke States and Geometry

Before we discuss physical consequences of the Hamiltonian, first we need to understand the Hilbert Space where everything is living a little bit better. The states in Chapter 1. composing spin-$\frac{1}{2}$ particles have the Pauli matrices as the basis of the algebra along with the identity. These correspond to the Lie group $\mathcal{SU}(2)$ which are isomorphic to the sphere. However, by merely

moving from n=2 to n=3 the group $\mathcal{SU}(3)$ and its corresponding algebra become a bit more complicated, I am not sure about the reader but we have a hard time visualizing an eight dimensional sphere where these states live. The nice aspect of such a large space is that it can be decomposed into many smaller spaces. If we pick a specific angular momentum level F, then provided the measurement times are faster than $1/\Gamma$ where Γ is the scattering rate, then the system will remain in the same manifold. Algebraically, this means that we are working in a symmetric subspace, which is well described in terms of Dick-States. The reason we can ultimately use these states, is because $\mathcal{SU}(3)$ can be decomposed into several representations which are isomorphic to $\mathcal{SU}(2)$. Through various combinations of basis matrices of $\mathcal{SU}(3)$ we can create symmetric spaces that are algebraically the same as the spin-1/2 algebra. If we fix a specific angular momentum then we are projecting from our total space into one of these spaces. The spin-1 algebra is span$\{F^2, F_z, F_+, F_-\}$. We can then develop how these act on the angular momentum states

$$\begin{aligned} F^2 \left|F,m\right\rangle &= F(F+1)\left|F,m\right\rangle \\ F_z \left|F,m\right\rangle &= m\left|F,m\right\rangle \\ F_\pm \left|F,m\right\rangle &= \sqrt{F(F+1)-m(m\pm 1)}\left|F,m\pm 1\right\rangle \end{aligned} \tag{4.7}$$

Where the allowed values of F are $\{\mathcal{N}, \mathcal{N}-1, \mathcal{N}-2, ...0\}$ and m_f is constrained to be $\{-F, ..0, ..F\}$.In the following section we will utilize these relations to explicitly derive the manifold of states for two atoms and demonstrate how to connect the angular momentum description with the standard computational basis.

4.2.2 Two-atom Spin-1 Dicke-States

The symmetric manifold used is $F = \mathcal{N}$ where N is the total number of atoms, so for $\mathcal{N} = 2$ there will be three manifolds, $F = 2, F = 1, F = 0$. Once we define the relations for these states, we will determine the construction of Atomic-spin cat states for the $F = 2$ manifold.When constructing a space of eigenvectors for an algebra, we have to first specify either the lowest weight or highest weight state. Then by repeated application of the raising or lowering operator we can

construct a ladder of states inside our Hilbert Space. For $\mathcal{N} = 2$ we start in the lowest weight and apply the raising operator and note that $m = n_+ - n_-$

$$\begin{aligned} F_+ \left|F = 2, m = -2\right\rangle &= F_+ \left|n_+ = 0, n_- = 2, n_0 = 0\right\rangle \\ \left|F = 2, m = -1\right\rangle &= \left|0, 1, 1\right\rangle \\ \left|F = 2, m = 0\right\rangle &= \frac{1}{\sqrt{3}} \left|1, 1, 0\right\rangle + \sqrt{\frac{2}{3}} \left|0, 0, 2\right\rangle \\ \left|F = 2, m = 1\right\rangle &= \left|1, 0, 1\right\rangle \\ \left|F = 2, m = 2\right\rangle &= \left|2, 0, 0\right\rangle \end{aligned} \tag{4.8}$$

Where in the above the left-hand side represents the angular momentum states, and the right hand side are the number states for the field. We can then translate this in terms of the basis, $\left|+\right\rangle, \left|-\right\rangle, \left|0\right\rangle$ resulting in

$$\begin{aligned} \left|F = 2, m = -2\right\rangle &= \left|--\right\rangle \\ \left|F = 2, m = -1\right\rangle &= \frac{\left|-0\right\rangle + \left|0-\right\rangle}{\sqrt{2}} \\ \left|F = 2, m = 0\right\rangle &= \frac{1}{\sqrt{3}} \left(\frac{\left|+-\right\rangle + \left|-+\right\rangle}{\sqrt{2}}\right) + \sqrt{\frac{2}{3}} \left|00\right\rangle \\ \left|F = 2, m = 1\right\rangle &= \frac{\left|+0\right\rangle + \left|0+\right\rangle}{\sqrt{2}} \\ \left|F = 2, m = 2\right\rangle &= \left|++\right\rangle \end{aligned} \tag{4.9}$$

Using this iterative method we repeat for the other two manifolds $N = 1$

$$\begin{aligned} \left|F = 1, m = -1\right\rangle &= \frac{\left|-0\right\rangle - \left|0-\right\rangle}{\sqrt{2}} \\ \left|F = 1, m = 0\right\rangle &= \frac{\left|+-\right\rangle - \left|-+\right\rangle}{\sqrt{2}} \\ \left|F = 1, m = 1\right\rangle &= \frac{\left|+0\right\rangle - \left|0+\right\rangle}{\sqrt{2}} \end{aligned} \tag{4.10}$$

And finally for $\mathcal{N} = 0$

$$|F = 0, m = 0\rangle = -\frac{1}{\sqrt{3}}\left(\frac{|+-\rangle + |-+\rangle}{\sqrt{2}}\right) + \frac{1}{\sqrt{3}}|0,0\rangle \tag{4.11}$$

Furthermore, we have constructed the spin-1 Dicke like states for the case of $\mathcal{N} = 2$. One can verify that each of these manifolds are orthogonal to one another, and properly normalized. One can extend this procedure further and derive a correspondence between the case of $\mathcal{N}$ atoms, but it tedious and one must worry about convergence properties when determining the Clebsch-Gordon, however, a calculation is presented in [49, 50, 51]. For the remaining section of the thesis we focus on the dynamics of the decoherence free subspace of $\mathcal{N} = 2$.

Decoherence is a persistent problem of quantum information, a non-unitary process, that introduced through heating effects causes rapid decay of the off-diagonal elements of the density matrix. This process is harmful when trying to engineer methods for information storage, creation of entangled states, or precision measurements. For optical systems the noise is primarily introduced through spontaneous emission. However, as mentioned above, this system takes place in a decoherence free subspace. These spaces are special because they are in principle exempt from decoherence due to a particular symmetry in the environment. Given a state in these subspaces they will all acquire the same phase under evolution so that any superposition of them remains intact despite environmental influences. In our system the environmental factor we should worry about is spontaneous emission. We already have adiabatically removed the excited state and transitions between the ground state levels are all forbidden and only occur through spin-flips mediated by virtual photons. Thus any superposition of states are going to be protected in this manifold from spontaneous emission.

4.2.3 Spin-1 Cats in a Symmetric Subspace

In chapter 1 of this work we dedicated time to develop a Quantum Zoo of states. One of which was the atomic cat states from non-linear time evolution. In this section we demonstrate that our effective spin-spin interaction can create these states provided we work in a symmetric manifold

at a fixed angular momentum. One purpose for making this constraint is that in this subspace the geometry is governed by $\mathcal{SU}(2)$, where the standard coherent states are defined. We could utilize $\mathcal{SU}(3)$ coherent state but the parameterization requires seven independent angles and the analytic expression is not insightful[52, 53]. It is common in high energy physics to use these types of states, but the basis they generally utilize is the Gelfand-Tsetlin basis[54, 55].

Beginning with the effective Hamiltonian in the beginning section we rewrite in a different form using the angular momentum algebra

$$\begin{aligned} H_{eff} &= \frac{|\Omega\epsilon_y/2|^2}{\kappa^2+\delta^2}\left(\frac{F_+F_-}{\Delta_-}+\frac{F_-F_+}{\Delta_+}\right) \\ &= \frac{|\Omega\epsilon_y/2|^2}{\kappa^2+\delta^2}\left(\frac{F_+F_-\Delta_+}{\Delta_-\Delta_+}+\frac{F_-F_+\Delta_-}{\Delta_+\Delta_-}\right) \\ &= \frac{|\Omega\epsilon_y/2|^2}{\kappa^2+\delta^2}\left(\frac{(F^2-F_z^2+F_z)\Delta_+}{\Delta_-\Delta_+}+\frac{(F^2-F_z^2-F_z)\Delta_-}{\Delta_+\Delta_-}\right) \\ &= \frac{|\Omega\epsilon_y/2|^2\delta}{(\kappa^2+\delta^2)(\omega_z^2+\delta^2)}\left(F^2-F_z^2+\beta F_z\right) \\ &= \chi\left(F^2-F_z^2+\beta F_z\right) \end{aligned} \tag{4.12}$$

To get line four from three above, we expanded the definitions of the detuning, and factored the equation which resulted in the constant, $\beta = \frac{\omega_z}{\delta}$, and χ is the coupling. We take the initial state of the atoms to be in spin-coherent state

$$|\theta,\phi\rangle = \sum_k \binom{2F}{k}^{1/2} sin^k\frac{\theta}{2}cos^{2F-k}\frac{\theta}{2}e^{-ik\phi}\,|F,k-F\rangle \tag{4.13}$$

Evolving the initial state under the Time-Dependent Schrodinger equation results in the following state

$$\begin{aligned} |\psi(t)\rangle &= \sum_k \binom{2F}{k}^{1/2} sin^k\frac{\theta}{2}cos^{2F-k}\frac{\theta}{2}e^{-ik\phi}e^{-it\chi(k(2F+1+\beta)+F(1-\beta))}e^{it\chi k(k+1)}\,|F,k-F\rangle \\ &= \sum_k \binom{2F}{k}^{1/2} sin^k\frac{\theta}{2}cos^{2F-k}e^{-ik\phi'}e^{i\frac{\pi}{m}\psi}e^{i\frac{\pi}{m}\chi k(k+1)}\,|F,k-F\rangle \end{aligned} \tag{4.14}$$

In the above derivation we set, $\tau = \chi t = \frac{\pi}{m}$ where m is an integer. We also defined the phases $\phi^{'} = \phi + \frac{\pi}{m}(2F + 1 + \beta)$ and $\psi = F(1 - \beta)$. We note that in the limit where $\beta = 1$ we have the same expressions as in the spin-$\frac{1}{2}$ case. In chapter 1, we demonstrated that the unitary operator, $U = e^{i\frac{\pi}{m}k(k+1)}$ is periodic for odd and even m. Following the same approach and expression from the Chapter 1, we determine the even and odd Atomic Schrodinger Cat states to be

$$\begin{aligned} |\psi_{odd}\rangle &= e^{-i\frac{\pi\psi}{m}} \sum_{q=0}^{m-1} f_q^{(o)} \left|\theta, \phi + \frac{\pi}{m}(2F + \beta + 1 - 2q)\right\rangle \\ |\psi_{even}\rangle &= e^{-i\frac{\pi\psi}{m}} \sum_{q=0}^{m-1} f_q^{(e)} \left|\theta, \phi + \frac{\pi}{m}(2F + \beta - 2q)\right\rangle \end{aligned} \tag{4.15}$$

When $\beta = 1$ the expression for the cat states above are equivalent to the Chapter 1 up to an overall phase. When first investigating properties of these states we demonstrated their utility in precision measurement of a phase. We sought to demonstrate the same abilities with these states, which would be experimentally more useful because they would have a longer coherence time since they live in a decoherence free subspace. A crucial part of that derivation was using the property, $\sigma_i^2 = 1$ where σ_i is a Pauli operator where we had to calculate e^{σ_i}. The problem is that in the $SU(3)$ basis, and spin-1 operators do not obey this relation, but rather, $e^{i\theta F_i} = 1 + isin(\theta)F_i + (cos(\theta) - 1)F_i^2$ where $i = x, y, z$. The evolution is non-trivial and initial calculation have shown that an analytical expression may not be insightful and is left to future work.

4.2.4 Entangled Two-Atom State

The previous section demonstrated the evolution under the effective Hamiltonian in a fixed angular momentum subspace gives rise to entangled superpositions of spin coherent states. Naturally, what happens if we allow the angular momentum spaces to mix upon evolution? That is the idea we address in this final section. First we fix some notation to distinguish between the angular momentum state and computation state. For the orbital levels, m_f, when in the zero level it will be denoted as $|F, m = 0\rangle$. When in the computational basis the state, $|0\rangle$ will be given $\left|\tilde{0}\right\rangle$ so as to not be confused. We will now use the construction from section 3.2.2 for the two atom states and

study their evolution. Consider the spin-1 atoms initially in the Zeeman sublevel,

$$\left|\tilde{0},\tilde{0}\right\rangle = \frac{1}{\sqrt{3}}\left|0,0\right\rangle + \sqrt{\frac{2}{3}}\left|2,0\right\rangle \tag{4.16}$$

Then evolving under the time-dependent Schrodinger equation using the effective Hamiltonian from the previous section

$$\begin{aligned}\left|\psi(t)\right\rangle &= \frac{1}{\sqrt{3}}\left|0,0\right\rangle + e^{-6i\chi t}\sqrt{\frac{2}{3}}\left|2,0\right\rangle \\ &= \left(\frac{e^{-6i\chi t}}{3} - \frac{1}{3}\right)\left(\left|+-\right\rangle + \left|-+\right\rangle\right) + \left(\frac{2e^{-6i\chi t}}{3} + \frac{1}{3}\right)\left|\tilde{0},\tilde{0}\right\rangle\end{aligned} \tag{4.17}$$

Here we used the definition of $|0,0\rangle$ and $|2,0\rangle$ in terms of the Zeeman levels which was derived in 4.2.2. Note that when $t = 0$ we recover the initial state as expected. The motivation for studying these states was from a recent experiment where the group was able to generate all nine Bell states for three levels and perform quantum teleportation[56]. Unlike the standard Bell states constructed with qubits, the added third level adds non-trivial phases to the states, and we were curious if we would be able to generate them for two atoms. We are able to generate states similar at various times, however, we are unable to generate the whole space because as can been seen above we cannot create combinations with terms, $|++\rangle$, and $|--\rangle$.

In the case of two atoms there are variety of tools developed in the context of quantum information to study the entanglement between bipartite systems, a few being; concurence[57], and Schmidt decomposition[58]. We look at the Schmidt coefficients, from which we can calculate the Schmidt number which is the number of nonzero coefficients for the decomposed state[58]. We calculate this for time evolved states at various χt to quantify the entanglement. In the appendix we give a summary on the theory of Schmidt decomposition for pure states. In the following we give an explicit calculation for $\chi t = \frac{\pi}{6}$

$$\left|\psi\right\rangle = \frac{-2}{3}\left(\left|+-\right\rangle + \left|-+\right\rangle\right) - \frac{1}{3}\left|\tilde{0},\tilde{0}\right\rangle \tag{4.18}$$

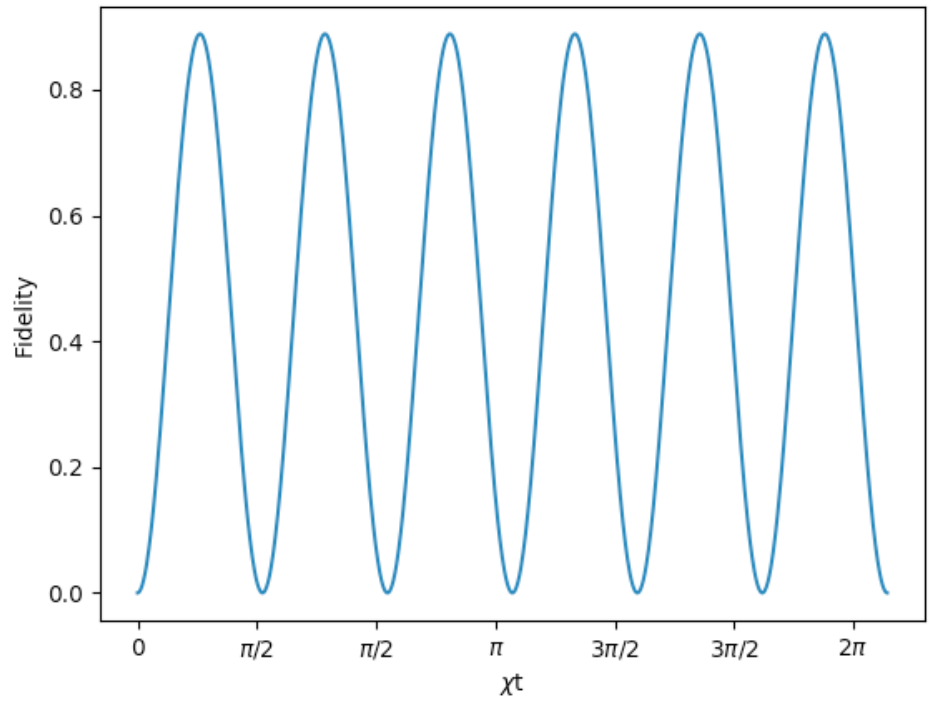

Figure 4.2: Fidelity of the time-evolved state against $|\phi\rangle = \frac{1}{\sqrt{2}}(|+-\rangle + |-+\rangle)$. Where, $\mathcal{F} = |\langle\phi|\psi(t)\rangle|^2$. For time $\chi t = \frac{\pi}{6}$ the fidelity is nearly 1, which is max entanglement confirming our findings from the Schmidt coefficients.

The first step is to determine the density matrix for this state

$$\begin{aligned}\rho = \frac{2}{9}|+-\rangle\langle\tilde{0},\tilde{0}| + \frac{4}{9}|+-\rangle\langle+-| \\ + \frac{4}{9}|+-\rangle\langle-+| + \frac{2}{9}|-+\rangle\langle\tilde{0},\tilde{0}| \\ + \frac{4}{9}|-+\rangle\langle+-| + \frac{4}{9}|-+\rangle\langle-+| \\ + \frac{1}{9}|\tilde{0},\tilde{0}\rangle\langle\tilde{0},\tilde{0}| + \frac{2}{9}|\tilde{0},\tilde{0}\rangle\langle+-| + \frac{2}{9}|\tilde{0},\tilde{0}\rangle\langle-+| \quad (4.19)\end{aligned}$$

The total Hilbert space $H = H_A \bigotimes H_B$ is the tensor product of the space for the individual atoms each of which is spanned by three possible states. To decompose we now find the partial trace for each subsystem

$$\begin{aligned}\rho_A &= Tr_B(\rho) \\ &= \frac{4}{9}\left|+\right\rangle\left\langle+\right| + \frac{4}{9}\left|-\right\rangle\left\langle-\right| + \frac{1}{9}\left|\tilde{0}\right\rangle\left\langle\tilde{0}\right| \\ &= Tr_A(\rho) \\ &= \rho_B\end{aligned} \tag{4.20}$$

Here we used $Tr(|i\rangle\langle j|) = \delta_{ij}$, and find the reduced density matrices are equivalent after tracing out the other system. We observe that the above matrix is diagonal with eigenvalues, $\lambda_1 = 4/9$, $\lambda_2 = 4/9$, $\lambda_3 = 1/9$. Then following the appendix the Schmidt coefficients are determined by the square root of the eigenvalues. Notice, how we have a degenerate eigenspace, this implies that the decomposition is not unique, we can find many basis to describe the state. This state contains 3 Schmidt coefficients implying that it is entangled due to being larger than one. We confirm the entanglement in another manner using the Fidelity see 4.2. The quantum fidelity is a measure of "distance" from a reference state to the one of interest, our fiducial state is taken to be $|\phi\rangle = \frac{1}{\sqrt{2}}(|+-\rangle + |-+\rangle)$ and the fidelity is found to be

$$\begin{aligned}\mathcal{F} &= |\langle\phi|\psi(t)\rangle|^2 \\ &= \frac{4}{9}(1 - cos(6\chi t))\end{aligned} \tag{4.21}$$

The 4.2 displays the behavior of the fidelity is periodic, at the points where it is maximum, the distance between the time-evolved state and the reference is minimal. These points are occurring for the states of highest Schmidt number indicating further the degree of entanglement.

In this chapter we were attempting to address the question of what is the particular regime where spin-exchange interaction can be realized? And what type entangled states can be created? We demonstrated that provided the cavity frequency is dominating compared to a weak drive field we can adiabatically eliminate the cavity mode resulting in an effective Hamiltonian that described a spin-flip process. More so, in a decoherence free subspace of fixed angular momentum, arbitrary coherent superpositions of atomic states can be realized which are robust to spontaneous emission. We further demonstrated that when the angular momentum states are allowed to mix we are able to

generate highly entangled states which we quantified through their Schmidt number and fidelity. In the final chapter we apply this the Hamiltonian on different grounds and see what phenomena can be realized when on Raman resonance. We primarily focus on the application of electromagnetically induced transparency which is has a wide range of applications for quantum informational purposes.

5. ELECTROMAGNETICALLY INDUCED TRANSPARENCY

With the advent of increasing technological capabilities studying information in the context of quantum many-body systems has become more accessible. An issue with quantum information processing is storing and retrieving information. This arises in atomic systems by transferring quantum states of light into metastable states of matter. A process well studied that achieves this mechanism is electromagnetically induced transparency(EIT)[25, 8]. This technique of eliminating the absorption of a medium is discussed in the classical setting in the first section. The unique result of EIT is that it can slow the group velocity of light propagating in the medium[37], which leads to the use of slow light for informational purposes. Since EIT first being discovered in optical mediums, it has since been applied in a varying of contexts such as; optomechanically-induced transparency [59, 60], and meta-materials with plasmons[61]. Optomechanical interactions are described by exceptionally non-linear Hamiltonians[62, 16, 63]. In section 2 we discuss how under a Holstein-Primakoff transformation our effective Hamiltonian from Chapter 2, takes on a similar non-linear structure. Using this formalism we then present the transparency conditions for this model and give an interpretation for the physical consequences.

5.1 Electromagnetically Induced Transparency

Why is an object black? The reason is that the medium absorbs all wavelengths of light. Suppose you want to make this dark medium clear now, how can this be accomplished? The unintuitive answer is to shine more light on it. This the natural phenomena of electromagnetically induced transparency. Given an otherwise opaque medium can be made transparent by adding a coupling laser to the system. Electromagnetically induced transparency is an on resonant behavior, i.e when the frequency of light is matched to an atomic transition frequency. If this matching occurs the propagating light is accompanied by strong absorption or dispersion, however, there are scenarios where the absorption can be cancelled. EIT is the result of the correct conditions leading to the cancellation of the absorption turning the medium opaque. Ultimately, this is a re-

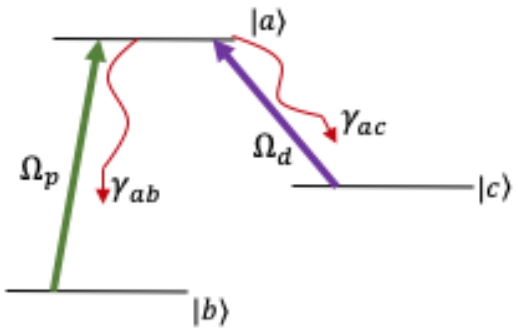

Figure 5.1: Lambda structure three-level atom, where the transition $|b\rangle$ to $|a\rangle$ is coupled by a weak probe field(green). While the transition $|c\rangle$ to $|a\rangle$ is coupled by a strong drive field(purple). The decay rates from the excited states are shown by the red-lines.

sult of the quantum states between the transitions destructively interfering. The first experimental realization[64] found that an optically thick medium becomes transparent to a weak probe field by applying an additional strong drive. Recently EIT has been applied to a wide range of more complex systems such as magneto-optical rotation [65], selective sub-radiance in atomic arrays[66], and at exceptional point in a coupled resonator[67].

5.1.1 Three-Level Atom

We consider an atomic system consisting of 3-level Λ as shown in 5.1. The ground state, $|b\rangle$ is coupled to $|a\rangle$ by a probe field with Rabi frequency Ω_p. While the excited state $|a\rangle$ and meta-stable state $|c\rangle$ are coupled by a drive field with a Rabi frequency Ω_d. The question we want to answer is, what is the dipoles' response to the probe field in the presence of the drive field? The probe field is weak compared to the drive, $\Omega_d \gg \Omega_p$. The combined effect of these fields is cause a superposition of the ground and meta-stable state which dresses the excited state.

$$H = \sum_{i=a,b,c} \omega_i \left|i\right\rangle \left\langle i\right| - \left(\Omega_p \left|a\right\rangle \left\langle b\right| e^{-i\omega_p t} + \Omega_d \left|a\right\rangle \left\langle c\right| e^{-i\omega_d t}\right) + H.C \tag{5.1}$$

Here ω_p and ω_d are respectively the frequency of the probe and drive field. To understand the coherent behavior we treat the system using a density matrix formalism. The reason for doing this

is that the off diagonal elements, ρ^{ij} relay the relative phases between the different states, where as, the diagonal components deliver information on the population statistics. The density matrix is given by the Von-Neumann equation

$$\dot{\rho} = -i[H, \rho] \tag{5.2}$$

Treating the system to be closed we add the incoherent decay in a phenomenological manner. If the atoms are initially in $|b\rangle$, then there will be few excitations that reach the upper level or the meta-stable state through emission due to the probe beam being too weak, therefore, $\rho^{aa} \approx 0$, $\rho^{cc} \approx 0$, and $\rho^{bb} \approx 1$. We are interested in the response of the probe field, thus, we want to density matrix element for the coherence between the states $|b\rangle$ and $|a\rangle$

$$\rho^{ab} = \frac{i\Omega_p e^{-i\omega_p t}(\gamma_{cb} + i\Delta)}{[(\gamma_{ab} + i\Delta)(\gamma_{cb} + i\Delta) + \Omega_d^2]} \tag{5.3}$$

Here $\Delta = \omega_{ab} - \omega_p$. To derive the equation above we find the equation of motion for each coherence and then since, Ω_p is weak it can be treated perturbatively while Ω_d is large it must be kept to all orders. Following this we make the substitutions, $\rho^{ab} = \tilde{\rho_{ab}} e^{-i\omega_p t}$, and $\rho^{cb} = \tilde{\rho_{cb}} e^{-i(\omega_p + \omega_{ca})t}$ into the equations of motion and solve the coupled differential equations.

To get an understanding of the relationship between the transmission and absorption of light we can use Beer-Lambert law which tells us that the transmission will be proportional to absorption and path length of medium

$$\mathcal{T}(\Delta) = e^{-Im[\chi]kL} \tag{5.4}$$

Where χ is the susceptibility which is a complex number. This is found through the relation to the polarization of a medium, $\mathcal{P} = \epsilon_0 \chi \mathcal{E}$. From the above relation we can deduce that the absorption is proportional to the imaginary part of χ. EIT then arises when the resonance condition is met, $\Delta = 0$, and in this case the real part of χ will vanish, and $Im(\chi)$ will be on the order of

γ_{cb}. Therefore, the ideal EIT condition is the limit where the decay of coherence between the ground level and meta-stable state vanish, which is a physical scenario since that transition is dipole forbidden. In this limit the transmission will go to unity, and absorption will go to zero. Furthermore, due to the presence of a drive field the system becomes transparent to the probe field.

The above section was not to give a rigorous demonstration of an already well studied model, but to give an overview of the classical theory for us to refer back on when describing the consequences of our system. Before moving on to our results, we first discuss transparency in optomechanical systems. The reason for this is that the structure of our Hamiltonian mimics the ones typically found in this discipline allowing us to apply these techniques to our problem.

5.1.2 Induced EIT with Optomechanics

The platform for optomechanics is different than everything discussed in this thesis thus far. Before now we have simply stated that the story is playing out in a linear resonator with a resonant frequency, ω_c. However, with optomechanics we consider a cavity that has a free hanging mirror, or connected to spring see 5.2. Vibrations result from the field impinging on the free-mirror causing the cavity resonance frequency to become dependent on the position of the swaying mirror, i.e $\omega_c = \frac{\pi n c}{L}(1 - \frac{x}{L})$, where L is the length of the cavity in equilibrium, c is the speed of light, and n is an integer. The Hamiltonian of the system can be described with the following structure[68, 69]

$$H = \omega_c a^\dagger a + \omega_m b^\dagger b + g(b^\dagger + b)a^\dagger a + i\epsilon_p(a^\dagger e^{-i\omega_p t} - a e^{i\omega_p t}) + i\epsilon_d(a^\dagger a^{-i\omega_d t} - a e^{i\omega_d t}) \qquad (5.5)$$

Here the a are the operators for the cavity field, b are the phonon operators. Then there is an applied probe and drive field just as in the case for atomic EIT, these are accompanied by the amplitudes, ϵ_p and ϵ_d. To tease out the EIT behavior we study the mean response of the probe field in the presence of the drive and therefore the quantum fluctuations are not examined. It is important to also be working in the sideband resolved limit where the frequency of the oscillator, $\omega_m \gg \kappa$ where κ is the cavity linewidth, this is the regime where normal mode splitting is known to occur[70, 71]. In this model the presence of the probe and drive field cause a radiation pressure force to oscillate at a

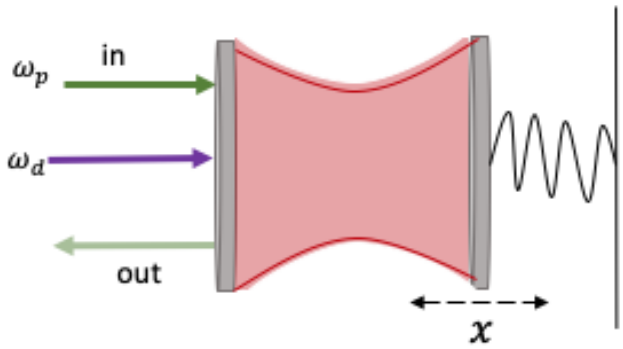

Figure 5.2: An optomechanical system consisting with a cavity field(red) and a mirror with a moveable boundary. The response of the driven system is then probed with a weak beam where its output response is measured.

difference of the two fields. If this is driven on resonance with frequency of the mechanical mode then the free standing mirror will coherently vibrate creating sidebands of the cavity fields. Due to the sideband resolved regime the anti-stokes scattering is the important contribution, because the Stokes scattering will be strongly depressed. When this scattering frequency matches that of the near-resonant probe field there will be destructive interference, causing the transparency.

5.2 Spin-1 Electromagnetically Induced Transparency

In Chapter 2 and 3 we developed a methodology for constructing effective many-body spin Hamiltonian when in the dispersive regime. The main underlying assumption was that certain frequency scales had to be far off the two-photon Raman resonance to apply the method of time averaging[3]. Here we are dealing with the same system, we are in a far detuned regime with respect to the cavity field and atomic transition. We know the atom-light interaction takes the form of the Faraday rotation as described previously. In developing the spin-spin exchange we had to make a second approximation comparing, Δ_+, Δ_- and $\Delta_+ \pm \Delta_-$. This final approximation is what allowed elimination of the cavity field, by assuming these combinations are large compared to the drive amplitude. In this chapter we are investigating the opposite regime which is where we are on the two-photon Raman resonance, $\Delta_+ = -\omega_z$. We show that the effective Hamiltonian in this case is similar to Eq 5.5 for the optomechanical situation, and we investigate the implications

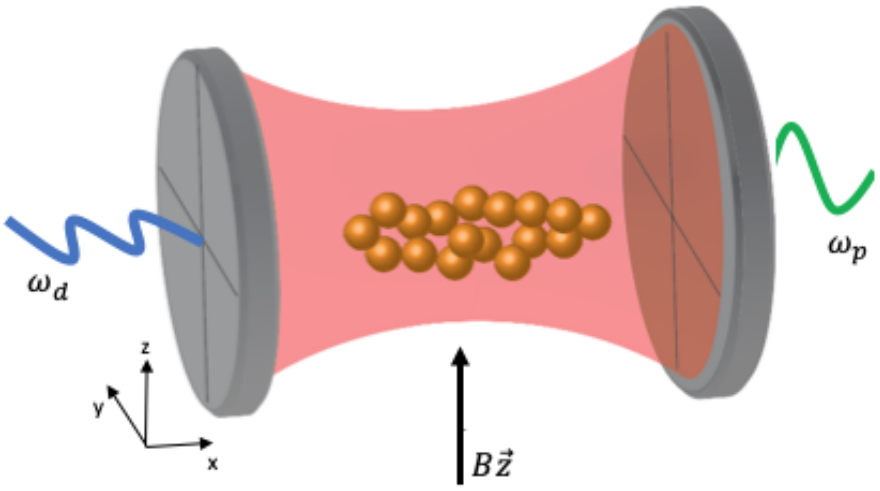

Figure 5.3: Linear cavity supporting a single cavity mode(red) with an ensemble of spin-1 atoms(orange). There is an applied probe beam(green) of frequency ω_p and strong drive field(blue) with frequency ω_d. The probe field is polarized in z, while the drive is in y. The black arrow indicates the perpendicular static magnetic field.

of EIT for this system.

5.2.1 Model

We consider a linear cavity with an ensemble of spin-1 atoms with the cavity field is propagating in x with polarization in y and z, along with an applied perpendicular magnetic field see 5.3. The drive field has an amplitude of $\epsilon_y = \sqrt{\frac{2\kappa_y \mathcal{P}_d}{\hbar\omega_d}}$, where $\mathcal{P}_d$ is the drive power, and ω_d is the frequency. In order see EIT effects we apply a weak probe field with an amplitude, $\epsilon_z = \sqrt{\frac{2\kappa_z \mathcal{P}_p}{\hbar\omega_p}}$, where $\mathcal{P}_p$ is the probe power, and ω_p the frequency. The system is described by the Hamiltonian

$$\begin{aligned} H_{AL} &= \frac{-g^2}{2i\Delta}(a_z^\dagger a_y + a_y^\dagger a_z)(F_+ - F_-) \\ H_B &= -\omega_z F_z \\ H_d &= i\epsilon_y(a_y^\dagger e^{-i\omega_d t} - a_y e^{i\omega_d t}) \\ H_p &= i\epsilon_z(a_z^\dagger e^{-i\omega_p t} - a_z e^{i\omega_p t}) \\ H_f &= \omega_c(a_y^\dagger a_y + a_z^\dagger a_z) \end{aligned} \tag{5.6}$$

To see how the Hamiltonian admits a similar structure as the optomechanical interaction we make a transformation of the spin variables. Consider the boson creation and annihilation operators which live on an infinite dimensional Fock space. The spin-1 operators must satisfy that angular momentum algebra, and this must be preserved under any transformation. The Holstein-Primakoff transformation[72] performs a truncation of the Fock space by mapping the spin-operators into the bosonic ones for large spin number. The spin variables take the form, $F_+ = \sqrt{2SN}b$, $F_- = \sqrt{2SN}b^\dagger$ and $F_z = (SN - b^\dagger b)$. One can show that the commutation relations, $[F_+, F_-] = 2F_z$ are held in this definition by noting, $[b, b^\dagger] = 1$. The atom-light interaction and Zeeman interaction are the only Hamiltonian's changed under this transformation

$$\begin{aligned} H_{AL} &= \frac{i\sqrt{2SN}g^2}{2\Delta}(a_z^\dagger a_y + a_y^\dagger a_z)(b - b^\dagger) \\ H_B &= \omega_z b^\dagger b \end{aligned} \tag{5.7}$$

Suppose the drive field is strong where, $\epsilon_y \gg \epsilon_z$ then we can treat the drive as a classical field in steady-state. To determine the field amplitudes, α_y, we determine the Heisenberg equations of motion for a_y in the absence of any interaction and set the time derivative to zero with the ansatz, $a_y = \alpha_y e^{-i\delta t}$

$$\begin{aligned} H_{int} &= i\Omega\left(a_z^\dagger \alpha_y b e^{-i(\delta+\omega_z)t} - a_z^\dagger \alpha_y b^\dagger e^{-i(\delta-\omega_z)t} + a_z \alpha_y^* b e^{i(\delta-\omega_z)t} - a_z \alpha_y^* b^\dagger e^{-i(\delta+\omega_z)t}\right) \\ H_p &= i\epsilon_z(a_z^\dagger e^{-i\delta_p t} - a_z e^{i\delta_p t}) \end{aligned} \tag{5.8}$$

Where above we also went into the interaction picture, resulting in the cavity-drive and cavity-probe detuning defined to be $\delta = \omega_d - \omega_c$ and $\delta_p = \omega_p - \omega_c$. The redefined coupling constant is, $\Omega = \frac{\sqrt{2SN}g^2}{2\Delta}$. Instead of making a dispersive approximation, we define the two-photon resonance conditions to be $\Delta_+ = \delta + \omega_z$ and $\Delta_- = \delta - \omega_z$. To develop EIT we set the two-photon Raman

resonance to zero resulting in the condition, $\delta = -\omega_z$

$$\begin{aligned} H_{int} &= i\Omega \left(a_z^\dagger \alpha_y b - a_z \alpha_y^* b^\dagger \right) \\ H_p &= i\epsilon_z (a_z^\dagger e^{-i\delta_p t} - a_z e^{i\delta_p t}) \end{aligned} \tag{5.9}$$

This resonance approximation also gives terms proportional to $e^{\pm 2i\omega_z t}$, which are off resonant and will not contribution to the dynamics, which is just the rotating-wave approximation[15]. To understand how the probe field responds in the presence of the coupling field, we determine the susceptibility through the equations of motion for, b and a_z.

$$\begin{aligned} \dot{a_z} &= \Omega \alpha_y b + \epsilon_z e^{-i\delta_p t} - \kappa_z a_z \\ \dot{b} &= -\Omega \alpha_y^* - \kappa_b b \end{aligned} \tag{5.10}$$

Here κ_z is the loss rate for the z-polarized cavity mode, and κ_b is the bosonic dampening. These equations are linear which allow an ansatz similar to when solving for the steady-state for the drive field. We assume the form to be, $a_z = \tilde{a} e^{-i\delta_p t}$ and $b = \tilde{b} e^{-i\delta_p t}$. Upon plugging these into the equations of motion the steady state fields satisfy

$$\begin{aligned} \tilde{a} &= \frac{\Omega \alpha_y \tilde{b}}{\kappa_z - i\delta_p} + \frac{\epsilon_z}{\kappa_z - i\delta_p} \\ \tilde{b} &= \frac{-\Omega \alpha_y^*}{\kappa_b - i\delta_p} \end{aligned} \tag{5.11}$$

Eliminating $\tilde{b}$ from the first equation above and solving for $\tilde{a}$, we determine the susceptibility to be

$$\begin{aligned} \chi &= \frac{2\kappa_z}{\epsilon_z} \tilde{a} \\ &= \frac{2\kappa_z}{(\kappa_z - i\delta_p) + \frac{|\Omega \alpha_y|^2}{\kappa_b - i\delta_p}} \end{aligned} \tag{5.12}$$

To visualize the response we look at the real and imaginary parts of the susceptibility which relay information on the dispersion and absorption of the output field at the probe frequency. The

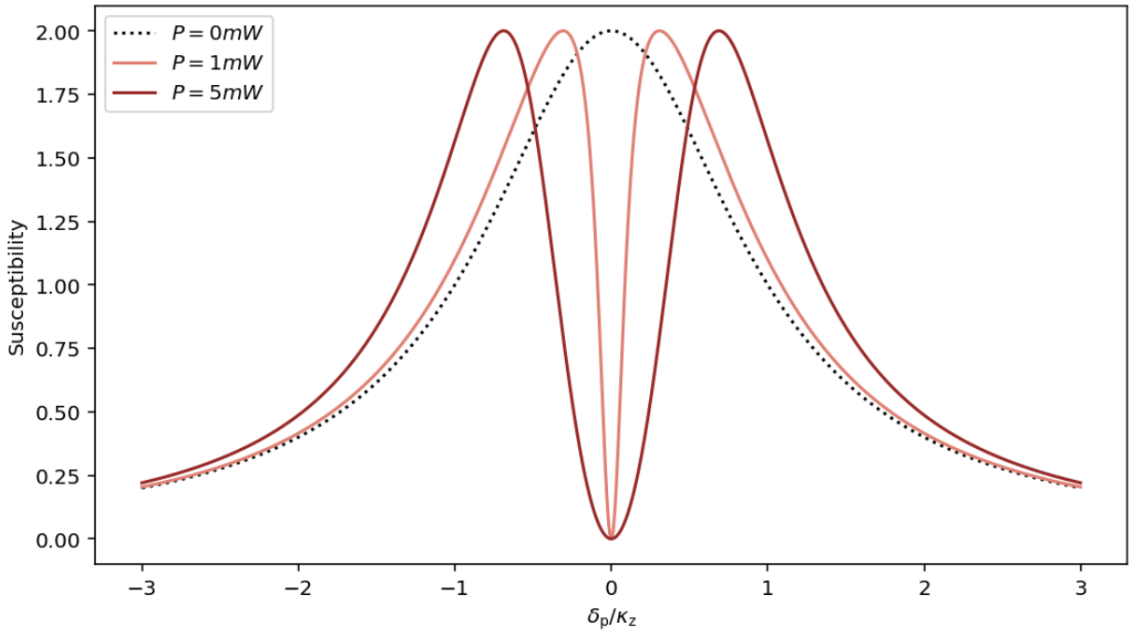

Figure 5.4: Real part of the susceptibility as a function of normalized frequency δ_p/κ_z. Demonstrating the behavior as the probe power is varied. The black dotted line is at $\mathcal{P}_d = 0$, coral at $\mathcal{P}_d = 1$ mW, and maroon at $\mathcal{P}_d = 5$ mW. The distinct EIT dip arises on the resonance demonstrating the emergence of a transparency window. Normal disperson becomes more apparent with increased probe powers.

susceptibility can be written as, $\chi = \chi_1 + i\chi_2$ where

$$\begin{aligned}\chi_1 &= \frac{2\kappa_z\kappa_b(\Omega^2\alpha_y^2 + \kappa_z\kappa_b - \delta_p^2) + 2\kappa_z\delta_p^2(\kappa_z + \kappa_b)}{(\Omega^2\alpha_y^2 + \kappa_z\kappa_b - \delta_p^2)^2 + \delta_p^2(\kappa_b + \kappa_z)^2} \\ \chi_2 &= \frac{2\kappa_z\kappa_b\delta_p(\kappa_z + \kappa_b) - \kappa_z\delta_p(\Omega^2\alpha_y^2 + \kappa_z\kappa_b - \delta_p^2)}{(\Omega^2\alpha_y^2 + \kappa_z\kappa_b - \delta_p^2)^2 + \delta_p^2(\kappa_b + \kappa_z)^2}\end{aligned} \tag{5.13}$$

To numerically simulate these expressions above we use the parameters from[6] to demonstrate applicability of our theory. We model the transition between, $\left|5S_{1/2}, F = 1\right\rangle$ to $\left|5P_{3/2}\right\rangle$ in a cloud of $N = 10^6$ rubidium-87 atoms trapped in a standing wave cavity with frequency, $\omega_c = 2\pi \times (4)10^{14}$ [38]. The atom-cavity resonance is far detuned, $\Delta = -2\pi \times 10$ GHZ. The length of the cavity, $l = 500\mu m$ with a Vacumm-Rabi frequency $2g = 2\pi \times 3.0(2.0)$ MHZ, $\kappa = 2\pi \times 200(50)$ kHz, and the cavity-drive detuning, $\delta = -2\pi \times 0.875$ MHZ. In the experiment they used a magnetic field of $4G$ which gives a Larmor frequency, $\omega_z = -70.4$MHZ which does not satisfy the necessary

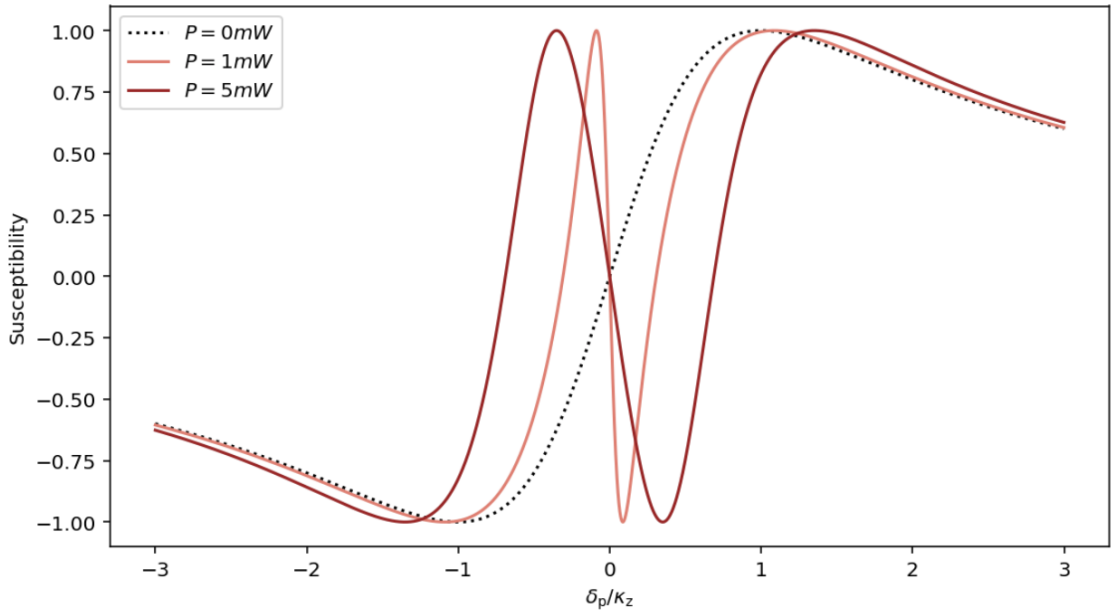

Figure 5.5: Imaginary part of the susceptibility as a function of the normalized frequency δ_p/κ_z. The dotted line is in the absence of the drive field. We then vary the probe power from 1mW(coral) to 5mW(maroon) and observe the distinct anomalous dispersion in the EIT region, leading to normal dispersion due to interference behavior.

condition. Therefore, to reach the EIT regime the magnetic field should be $B = 0.285$G.

In 5.4 we investigate the real part at various probe powers. We see that when the probe field is absent we return the standard Lorentzian behavior which signifies that there is complete absorption. As the power of the probe field is increased we see a narrow contribution that is inverted, which is the opening of the EIT window. With higher probe powers the dip will begin to broaden and demonstrate a normal dispersion which is accompanied with a reduction in the group velocity[73]. Contrasting with atomic-EIT the dip does not go all the way to zero in this case, because there is no infinite lifetime. In our model the "big oscillator" is a large ensemble of atoms in the ground state, and as discussed in previous chapters there is no decay between these atoms, which implies the oscillator has a zero dampening factor, i.e $\kappa_b = 0$, which would lead to larger coherence times facilitating better quantum memory, and light storage protocols. In 5.4 the nature of the dip is a result of destructive interference asymmetric profiles in the response function in the EIT region. In 5.5 we see that on resonance the complex susceptibility vanishes, which implies the refractive index

will go to unity and there will be perfect transmission of the probe field at the output, implying that the phase of the probe will be the same as if in vacuum. We also observe how that due to the drive field the anomalous dispersion is changed to normal. This behavior in the response function has been experimentally seen in a variety of systems[74, 75, 76].

In this final chapter we investigated a different aspect of the effective spin exchange Hamiltonian. Finding that when on resonance the ensemble of ground state atoms behave has a collective oscillator such that when a weak probe field, accompanied with a strong drive induces perfect transmission of the probe. Compared to the standard OMIT set-up our oscillator is not restricted by its dampening due to the absence of spontaneous emission. Furthermore, this model poses as a strong candidate for memory protocols, and state transfer in quantum simulations.

6. SUMMARY AND CONCLUSIONS

Not all time-scales are treated equal. Through the consideration of what the dominating dynamics are can result in a radically different description of the system as reflected through the Hamiltonian. In general solving the dynamics of a complete system is impossible, which is what makes effective interactions important. These descriptions are projections onto a subspace of the total system, reflecting a partial spectrum of the eigenstates. Previously researchers had to utilize projection operator methods to adiabatically eliminate degrees of freedom through the density operator. The method developed in this thesis is unique due to the simplicity. Our method requires only a simple integral, and algebraic manipulations to realize precise effective interactions. More so, our method works over multi-time scales. This is reflected in the application of spin-1 atoms, where in order to realize a description solely in terms of the atomic degrees of freedom, required two time averaging procedures. Each use had to weigh the dominating degree of freedom, and determine the correct regime to validly remove the fast dynamics. This development, is a step forward in understanding more complex many-body systems and how we may realize them in experimental settings.

Beyond the development of the technique of realizing many-body effective Hamiltonian's the system we choose to study is unique in its own right and has several advantages compared to the standard spin-$\frac{1}{2}$ system. Real atomic structures are hopelessly complicated, and experimentally realizing only two levels is a very specific goal. By understanding higher spins systems, we pave a way to study atoms in a more general setting. This theoretical description can easily be extended to $\mathcal{SU}(N)$ spin systems, allowing for precise modelling of more realistic atomic structures. Another key advantage of the spin-1 system is that by including more atomic levels, through the adiabatic elimination, we can constrain the dynamics to take place within a ground state manifold. These spaces are special because they are protected from decoherence resulting from spontaneous emission. The only worry comes from atomic collisions. However, this small issue can be taken care of if the sample of atoms is ultra-cold, and dilute.

We developed a hammer in this thesis, and the amount of nails left to be hit is uncountable. A few notable ones for investigation is the conversion of polarization of input probe beam into a different output polarization, known as magneto-optical rotation. Also, our specific spin-1 effective interaction can be mapped to a spin-1 Heisenberg model which is known to host interesting phase transitions, and special non-thermalizing eigenstates known as scarred states. More so, our method opens up a way to study interesting statistical properties of condensed matter systems, simulated in a quantum optically setting. Finally, through the demonstration of EIT it would be interesting to study collective state transfer in these decoherence-free subspaces, and compare the coherence time compared to standard methods.

APPENDIX A

TIME-AVERAGING

A.1 Introduction

The central tool used throughout this thesis was adiabatic elimination of certain degrees of freedom. The systems that we dealt with in this work are composed of an atomic and light field degree of freedom. In a particular problem the dynamics are occurring on the relevant time-scale, and depending on the regime other degrees may not be contributing and therefore you can trace them out of the Hilbert space. The standard method of this is by constructing the density-matrix and the dissipation terms, and then tracing out the degree of freedom[77]. When moving into the interaction picture the discrepancy of the time scale can arise through harmonically oscillating exponential. For this case there have been several methods put forward on adiabatic elimination[19, 18] which give the same effective theory as the method we put forward.

A.2 Method of Time Averaging

First, take the Hamiltonian to be the form, $H = H_0 + V(t)$, where H_0 is the free term and $V(t)$ is a perturbation. In this thesis the V was the dipole-atom interaction. Then by defining a unitary operator, $U = e^{-iH_0 t}$ move into the interaction picture. Upon this transformation the Hamiltonian will be of the form, $H_+ e^{-i\delta t} + H_- e^{i\delta t}$ where δ is the detuning depending on the form the Hamiltonian in the Schrodinger picture. If the exponential in each term are rapidly oscillating we can average time over time($\hbar = 1$)

$$\frac{\partial \psi}{\partial t} = -iV(t)\psi \tag{A.1}$$

Here $V(t)$ is a fast oscillating Hamiltonian in the interaction picture, where $\langle\psi| V |\psi\rangle = 0$. Now we break the state into a slow and fast part, $\psi = \overline{\phi} + \phi$, with $\overline{\phi}$, and ϕ being the time-averaged and rapidly oscillating components. Inserting this ansatz into the equation above and equate the fast

variables results in

$$\frac{\partial \phi}{\partial t} = -iV(t)\overline{\phi} \tag{A.2}$$

Integrating the above solution

$$\begin{aligned} \phi &= Te^{-i\int_0^t V(\tau)d\tau}\overline{\phi} \\ &= -i\int_0^t V(\tau)d\tau\overline{\phi} \end{aligned} \tag{A.3}$$

Here we go to first order in the interaction from the time-ordered Dyson series. With this solution we iterate it in the Schrodinger equation and equate the time-averaged variables which to first order gives

$$\begin{aligned} \overline{\phi} &= -i\left(\overline{-iV(t)\int_0^t V(\tau)d\tau}\right)\overline{\phi} \\ &= -iH_{eff}\overline{\phi} \end{aligned} \tag{A.4}$$

Where the effective Hamiltonian is the time-averaged and defined to be, $H_{eff} = \overline{-iV(t)\int_0^t V(\tau)d\tau}$. In general when determining the effective interaction this approach will result in a time-independent Hamiltonian since the fast oscillating portions will be sent to zero. However, it is important to understand the timescale that the dynamics are occurring because there are instances where you cannot just set the exponential parts to zero since they wont be in a fast oscillating regime, resulting in a time-dependent interaction.

APPENDIX B

SCHMIDT DECOMPOSTION

As pointed out throughout the thesis quantum information has the upper hand over classical information due to entanglement. This natural result is still far from being completely understood and the tools developed for quantifying the degree of entanglement only exist between bipartite systems. In this thesis we considered our subsystems to be two spin-1 atoms each containing three possible levels.The Hilbert space is then, $H = H_1 \bigotimes H_2$ with $dim(H) = 3^N$. Since this Hilbert space is finite dimensional then it is also Cauchy, which means that there is a notion of convergence for sequences. Therefore, we can write the state for the total system as[58]

$$|\psi\rangle = \sum_i \lambda_i |i_A\rangle \bigotimes |i_B\rangle \tag{B.1}$$

Here λ_i are positive and $\sum_i \lambda_i^2 = 1$ and are known as the Schmidt coefficients. To understand whether the state is a product state, we determine the density matrix for each subsystem, $\rho_A = Tr_B(\rho)$ and $\rho_B = Tr_A(\rho)$. What you find is

$$\begin{aligned} \rho_A &= \sum_i \lambda_i^2 |i_A\rangle \langle i_A| \\ \rho_B &= \sum_i \lambda_i^2 |i_B\rangle \langle i_B| \end{aligned} \tag{B.2}$$

The reduced density matrices share the same eigenvalues and the number of non-zero eigenvalues is the Schmidt number and quantifes the degree of entanglement. For example, is the state has a Schmidt number of one then it is pure and non-entangled. In this thesis we found depending on the point in time evolution that the max entanglement was found at a Schmidt number of 3.

REFERENCES

[1] S. Bernon, H. Hattermann, D. Bothner, M. Knufinke, P. Weiss, F. Jessen, D. Cano, M. Kemmler, R. Kleiner, D. Koelle, *et al.*, "Manipulation and coherence of ultra-cold atoms on a superconducting atom chip," *Nature communications*, vol. 4, no. 1, pp. 1–8, 2013.

[2] J. You and F. Nori, "Superconducting circuits and quantum information," *arXiv preprint quant-ph/0601121*, 2006.

[3] G. S. Agarwal and P. Pathak, "dc-field-induced enhancement and inhibition of spontaneous emission in a cavity," *Physical Review A*, vol. 70, no. 2, p. 025802, 2004.

[4] E. T. Jaynes and F. W. Cummings, "Comparison of quantum and semiclassical radiation theories with application to the beam maser," *Proceedings of the IEEE*, vol. 51, no. 1, pp. 89–109, 1963.

[5] M. A. Norcia, R. J. Lewis-Swan, J. R. Cline, B. Zhu, A. M. Rey, and J. K. Thompson, "Cavity-mediated collective spin-exchange interactions in a strontium superradiant laser," *Science*, vol. 361, no. 6399, pp. 259–262, 2018.

[6] E. J. Davis, G. Bentsen, L. Homeier, T. Li, and M. H. Schleier-Smith, "Photon-mediated spin-exchange dynamics of spin-1 atoms," *Physical review letters*, vol. 122, no. 1, p. 010405, 2019.

[7] E. J. Davis, A. Periwal, E. S. Cooper, G. Bentsen, S. J. Evered, K. Van Kirk, and M. H. Schleier-Smith, "Protecting spin coherence in a tunable heisenberg model," *arXiv preprint arXiv:2003.06087*, 2020.

[8] S. E. Harris, "Electromagnetically induced transparency," in *Quantum Electronics and Laser Science Conference*, p. QTuB1, Optical Society of America, 1997.

[9] M. Fleischhauer and C. Mewes, "Decoherence and decoherence suppression in ensemble-based quantum memories for photons," in *Quantum Information With Continuous Variables*

Of Atoms And Light, pp. 581–599, World Scientific, 2007.

[10] M. Fleischhauer and M. D. Lukin, "Dark-state polaritons in electromagnetically induced transparency," *Physical review letters*, vol. 84, no. 22, p. 5094, 2000.

[11] J. Huang, M. Zhuang, B. Lu, Y. Ke, and C. Lee, "Achieving heisenberg-limited metrology with spin cat states via interaction-based readout," *Physical Review A*, vol. 98, no. 1, p. 012129, 2018.

[12] C. Pope, *Electromagnetic Theory II*. Lecture Notes in Physics, College Station TX: Texas AM University, 2018.

[13] C. Pope, *General Relativity*. Lecture Notes in Physics, College Station TX: Texas AM University, 2018.

[14] P. Woit, Woit, and Bartolini, *Quantum theory, groups and representations*. Springer, 2017.

[15] C. Gardiner and P. Zoller, *The Quantum World of Ultra-Cold Atoms and Light Book I: Foundations of Quantum Optics*, vol. 2. World Scientific Publishing Company, 2014.

[16] J. Ma, X. Wang, C.-P. Sun, and F. Nori, "Quantum spin squeezing," *Physics Reports*, vol. 509, no. 2-3, pp. 89–165, 2011.

[17] H. Saito and M. Ueda, "Squeezed few-photon states of the field generated from squeezed atoms," *Physical Review A*, vol. 59, no. 5, p. 3959, 1999.

[18] O. Gamel and D. F. James, "Time-averaged quantum dynamics and the validity of the effective hamiltonian model," *Physical Review A*, vol. 82, no. 5, p. 052106, 2010.

[19] F. Reiter and A. S. Sørensen, "Effective operator formalism for open quantum systems," *Physical Review A*, vol. 85, no. 3, p. 032111, 2012.

[20] A. Sørensen and K. Mølmer, "Spin-spin interaction and spin squeezing in an optical lattice," *Physical review letters*, vol. 83, no. 11, p. 2274, 1999.

[21] R. Sewell, M. Koschorreck, M. Napolitano, B. Dubost, N. Behbood, and M. Mitchell, "Magnetic sensitivity beyond the projection noise limit by spin squeezing," *Physical review letters*, vol. 109, no. 25, p. 253605, 2012.

[22] F. Arecchi, E. Courtens, R. Gilmore, and H. Thomas, "Atomic coherent states in quantum optics," *Physical Review A*, vol. 6, no. 6, p. 2211, 1972.

[23] K. Tara, G. Agarwal, and S. Chaturvedi, "Production of schrödinger macroscopic quantum-superposition states in a kerr medium," *Physical Review A*, vol. 47, no. 6, p. 5024, 1993.

[24] R. W. Robinett, "Quantum wave packet revivals," *Physics Reports*, vol. 392, no. 1-2, pp. 1–119, 2004.

[25] G. S. Agarwal, *Quantum optics*. Cambridge University Press, 2012.

[26] T. Tilma, M. J. Everitt, J. H. Samson, W. J. Munro, and K. Nemoto, "Wigner functions for arbitrary quantum systems," *Physical review letters*, vol. 117, no. 18, p. 180401, 2016.

[27] T. Tilma and E. Sudarshan, "Generalized euler angle parametrization for su (n)," *Journal of Physics A: Mathematical and General*, vol. 35, no. 48, p. 10467, 2002.

[28] T. Tilma and K. Nemoto, "Su (n)-symmetric quasi-probability distribution functions," *Journal of Physics A: Mathematical and Theoretical*, vol. 45, no. 1, p. 015302, 2011.

[29] M. Brune, S. Haroche, J. Raimond, L. Davidovich, and N. Zagury, "Manipulation of photons in a cavity by dispersive atom-field coupling: Quantum-nondemolition measurements and generation of "schrödinger cat"states," *Physical Review A*, vol. 45, no. 7, p. 5193, 1992.

[30] C. C. Gerry and R. Grobe, "Generation and properties of collective atomic schrödinger-cat states," *Physical Review A*, vol. 56, no. 3, p. 2390, 1997.

[31] C. Song, K. Xu, H. Li, Y.-R. Zhang, X. Zhang, W. Liu, Q. Guo, Z. Wang, W. Ren, J. Hao, *et al.*, "Generation of multicomponent atomic schrödinger cat states of up to 20 qubits," *Science*, vol. 365, no. 6453, pp. 574–577, 2019.

[32] M. Gärttner, J. G. Bohnet, A. Safavi-Naini, M. L. Wall, J. J. Bollinger, and A. M. Rey, "Measuring out-of-time-order correlations and multiple quantum spectra in a trapped-ion quantum magnet," *Nature Physics*, vol. 13, no. 8, pp. 781–786, 2017.

[33] T. J. Elliott, W. Kozlowski, S. Caballero-Benitez, and I. B. Mekhov, "Multipartite entangled spatial modes of ultracold atoms generated and controlled by quantum measurement," *Physical review letters*, vol. 114, no. 11, p. 113604, 2015.

[34] A. Facon, E.-K. Dietsche, D. Grosso, S. Haroche, J.-M. Raimond, M. Brune, and S. Gleyzes, "A sensitive electrometer based on a rydberg atom in a schrödinger-cat state," *Nature*, vol. 535, no. 7611, pp. 262–265, 2016.

[35] R. McConnell, H. Zhang, S. Ćuk, J. Hu, M. H. Schleier-Smith, and V. Vuletić, "Generating entangled spin states for quantum metrology by single-photon detection," *Physical Review A*, vol. 88, no. 6, p. 063802, 2013.

[36] D. Leibfried, E. Knill, S. Seidelin, J. Britton, R. B. Blakestad, J. Chiaverini, D. B. Hume, W. M. Itano, J. D. Jost, C. Langer, *et al.*, "Creation of a six-atom 'schrödinger cat'state," *Nature*, vol. 438, no. 7068, pp. 639–642, 2005.

[37] G. S. Agarwal, R. Puri, and R. Singh, "Atomic schrödinger cat states," *Physical Review A*, vol. 56, no. 3, p. 2249, 1997.

[38] D. A. Steck, "Rubidium 87 d line data," 2001.

[39] L. LeBlanc and J. Thywissen, "Species-specific optical lattices," *Physical Review A*, vol. 75, no. 5, p. 053612, 2007.

[40] W. F. Holmgren, R. Trubko, I. Hromada, and A. D. Cronin, "Measurement of a wavelength of light for which the energy shift for an atom vanishes," *Physical review letters*, vol. 109, no. 24, p. 243004, 2012.

[41] B. Arora, M. Safronova, and C. W. Clark, "Tune-out wavelengths of alkali-metal atoms and their applications," *Physical Review A*, vol. 84, no. 4, p. 043401, 2011.

[42] A. Sommerfeld, *Electrodynamics: lectures on theoretical physics*, vol. 3. Academic Press, 2013.

[43] R. Sewell, M. Napolitano, N. Behbood, G. Colangelo, and M. Mitchell, "Certified quantum non-demolition measurement of a macroscopic material system," *Nature Photonics*, vol. 7, no. 7, p. 517, 2013.

[44] G. Colangelo, F. M. Ciurana, L. C. Bianchet, R. J. Sewell, and M. W. Mitchell, "Simultaneous tracking of spin angle and amplitude beyond classical limits," *Nature*, vol. 543, no. 7646, pp. 525–528, 2017.

[45] M. Jasperse, M. Kewming, S. Fischer, P. Pakkiam, R. Anderson, and L. Turner, "Continuous faraday measurement of spin precession without light shifts," *Physical Review A*, vol. 96, no. 6, p. 063402, 2017.

[46] G. A. Smith, S. Chaudhury, A. Silberfarb, I. H. Deutsch, and P. S. Jessen, "Continuous weak measurement and nonlinear dynamics in a cold spin ensemble," *Physical review letters*, vol. 93, no. 16, p. 163602, 2004.

[47] C. D. Hamley, C. Gerving, T. Hoang, E. Bookjans, and M. S. Chapman, "Spin-nematic squeezed vacuum in a quantum gas," *Nature Physics*, vol. 8, no. 4, pp. 305–308, 2012.

[48] K. Sun, C. Qu, Y. Xu, Y. Zhang, and C. Zhang, "Interacting spin-orbit-coupled spin-1 bose-einstein condensates," *Physical Review A*, vol. 93, no. 2, p. 023615, 2016.

[49] H. Pu, C. Law, S. Raghavan, J. Eberly, and N. Bigelow, "Spin-mixing dynamics of a spinor bose-einstein condensate," *Physical Review A*, vol. 60, no. 2, p. 1463, 1999.

[50] C. Law, H. Pu, and N. Bigelow, "Quantum spins mixing in spinor bose-einstein condensates," *Physical review letters*, vol. 81, no. 24, p. 5257, 1998.

[51] J. Heinze, F. Deuretzbacher, and D. Pfannkuche, "Influence of the particle number on the spin dynamics of ultracold atoms," *Physical Review A*, vol. 82, no. 2, p. 023617, 2010.

[52] K. Nemoto and B. C. Sanders, "Superpositions of su (3) coherent states via a nonlinear evolution," *Journal of Physics A: Mathematical and General*, vol. 34, no. 10, p. 2051, 2001.

[53] K. Nemoto, "Generalized coherent states for su (n) systems," *Journal of Physics A: Mathematical and General*, vol. 33, no. 17, p. 3493, 2000.

[54] A. Molev, "Gelfand-tsetlin bases for classical lie algebras," *arXiv preprint math/0211289*, 2006.

[55] J. Paldus, "Group theoretical approach to the configuration interaction and perturbation theory calculations for atomic and molecular systems," *The Journal of Chemical Physics*, vol. 61, no. 12, pp. 5321–5330, 1974.

[56] X.-M. Hu, C. Zhang, B.-H. Liu, Y.-F. Huang, C.-F. Li, and G.-C. Guo, "Experimental multilevel quantum teleportation," *arXiv preprint arXiv:1904.12249*, 2019.

[57] W. K. Wootters, "Entanglement of formation and concurrence.," *Quantum Information & Computation*, vol. 1, no. 1, pp. 27–44, 2001.

[58] M. A. Nielsen and I. Chuang, "Quantum computation and quantum information," 2002.

[59] A. H. Safavi-Naeini, T. M. Alegre, J. Chan, M. Eichenfield, M. Winger, Q. Lin, J. T. Hill, D. E. Chang, and O. Painter, "Electromagnetically induced transparency and slow light with optomechanics," *Nature*, vol. 472, no. 7341, pp. 69–73, 2011.

[60] S. Weis, R. Rivière, S. Deléglise, E. Gavartin, O. Arcizet, A. Schliesser, and T. J. Kippenberg, "Optomechanically induced transparency," *Science*, vol. 330, no. 6010, pp. 1520–1523, 2010.

[61] A. Hatef, S. M. Sadeghi, and M. R. Singh, "Plasmonic electromagnetically induced transparency in metallic nanoparticle–quantum dot hybrid systems," *Nanotechnology*, vol. 23, no. 6, p. 065701, 2012.

[62] A. Kronwald and F. Marquardt, "Optomechanically induced transparency in the nonlinear quantum regime," *Physical review letters*, vol. 111, no. 13, p. 133601, 2013.

[63] H. Xiong, L.-G. Si, A.-S. Zheng, X. Yang, and Y. Wu, "Higher-order sidebands in optomechanically induced transparency," *Physical Review A*, vol. 86, no. 1, p. 013815, 2012.

[64] K.-J. Boller, A. Imamoğlu, and S. E. Harris, "Observation of electromagnetically induced transparency," *Physical Review Letters*, vol. 66, no. 20, p. 2593, 1991.

[65] R. Duggan, J. del Pino, E. Verhagen, and A. Alù, "Optomechanically induced birefringence and optomechanically induced faraday effect," *Physical review letters*, vol. 123, no. 2, p. 023602, 2019.

[66] A. Asenjo-Garcia, M. Moreno-Cardoner, A. Albrecht, H. Kimble, and D. E. Chang, "Exponential improvement in photon storage fidelities using subradiance and "selective radiance" in atomic arrays," *Physical Review X*, vol. 7, no. 3, p. 031024, 2017.

[67] C. Wang, X. Jiang, G. Zhao, M. Zhang, C. W. Hsu, B. Peng, A. D. Stone, L. Jiang, and L. Yang, "Electromagnetically induced transparency at a chiral exceptional point," *Nature Physics*, pp. 1–7, 2020.

[68] G. S. Agarwal and S. Huang, "Electromagnetically induced transparency in mechanical effects of light," *Physical Review A*, vol. 81, no. 4, p. 041803, 2010.

[69] G. Agarwal and S. Huang, "Optomechanical systems as single-photon routers," *Physical Review A*, vol. 85, no. 2, p. 021801, 2012.

[70] S. Gröblacher, K. Hammerer, M. R. Vanner, and M. Aspelmeyer, "Observation of strong coupling between a micromechanical resonator and an optical cavity field," *Nature*, vol. 460, no. 7256, pp. 724–727, 2009.

[71] F. Marquardt, J. P. Chen, A. A. Clerk, and S. Girvin, "Quantum theory of cavity-assisted sideband cooling of mechanical motion," *Physical review letters*, vol. 99, no. 9, p. 093902, 2007.

[72] T. Holstein and H. Primakoff, "Field dependence of the intrinsic domain magnetization of a ferromagnet," *Physical Review*, vol. 58, no. 12, p. 1098, 1940.

[73] S. Harris, J. Field, and A. Kasapi, "Dispersive properties of electromagnetically induced transparency," *Physical Review A*, vol. 46, no. 1, p. R29, 1992.

[74] S. Zhang, D. A. Genov, Y. Wang, M. Liu, and X. Zhang, "Plasmon-induced transparency in metamaterials," *Physical review letters*, vol. 101, no. 4, p. 047401, 2008.

[75] N. Papasimakis, V. A. Fedotov, N. Zheludev, and S. Prosvirnin, "Metamaterial analog of electromagnetically induced transparency," *Physical Review Letters*, vol. 101, no. 25, p. 253903, 2008.

[76] D. D. Smith, H. Chang, K. A. Fuller, A. Rosenberger, and R. W. Boyd, "Coupled-resonator-induced transparency," *Physical Review A*, vol. 69, no. 6, p. 063804, 2004.

[77] C. Gardiner, P. Zoller, and P. Zoller, *Quantum noise: a handbook of Markovian and non-Markovian quantum stochastic methods with applications to quantum optics*. Springer Science & Business Media, 2004.